



PERGAMON

Journal of the Mechanics and Physics of Solids
50 (2002) 1897–1922

JOURNAL OF THE
MECHANICS AND
PHYSICS OF SOLIDS

www.elsevier.com/locate/jmps

The free energy of mixing for n -variant martensitic phase transformations using quasi-convex analysis

Sanjay Govindjee^{a,*}, Alexander Mielke^b, Garrett J. Hall^c

^a*Department of Civil and Environmental Engineering, Structural Engineering, Mechanics, and Materials, University of California, Berkeley, 721 Davis hall, Berkeley, CA 94720-1710, USA*

^b*Mathematisches Institut A, Universität Stuttgart, 70569 Stuttgart, Germany*

^c*Department of Civil Engineering, Clarkson University, Potsdam, NY 13699, USA*

Received 16 May 2001; received in revised form 8 January 2002; accepted 9 February 2002

Abstract

The construction of effective models for materials that undergo martensitic phase transformations requires usable and accurate functional representations for the free energy density. The general representation of this energy is known to be highly non-convex; it even lacks the property of quasi-convexity. A quasi-convex relaxation, however, does permit one to make certain estimates and powerful conclusions regarding phase transformation. The general expression for the relaxed free energy is however not known in the n -variant case. Analytic solutions are known only for up to 3 variants, whereas cases of practical interests involve 7–13 variants. In this study we examine the n -variant case utilizing relaxation theory and produce a seemingly obvious but very powerful observation regarding a lower bound to the quasi-convex relaxation that makes practical evolutionary computations possible. We also examine in detail the 4-variant case where we explicitly show the relation between three different forms of the free energy of mixing: upper bound by lamination, the Reuß lower bound, and a lower estimate of the \mathbb{H} -measure bound. A discussion of the bounds and their utility is provided; sample computations are presented for illustrative purposes. © 2002 Published by Elsevier Science Ltd.

Keywords: A. Shape memory alloy; Martensitic phase transformation; C. Quasi-convexity; \mathbb{H} -measures

* Corresponding author. Tel.: +1-510-642-6060; fax: +1-510-643-8928.

E-mail addresses: govindjee@ce.berkeley.edu (S. Govindjee), mielke@mathematik.uni-stuttgart.de (A. Mielke), gjhall@clarkson.edu (G.J. Hall).

1. Introduction

In the theory of shape memory alloys and other martensitic problems it is the basic assumption that each mesoscopic part of the crystal can choose to be in one of the n allowed phases. We distinguish these phases by their stored-energy densities

$$W(\boldsymbol{\varepsilon}, \mathbf{e}_i) = \frac{1}{2}(\boldsymbol{\varepsilon} - \boldsymbol{\varepsilon}_i) : \mathbb{C}_i : (\boldsymbol{\varepsilon} - \boldsymbol{\varepsilon}_i) + \alpha_i, \quad i = 1, \dots, n,$$

where $\mathbf{e}_i \in \mathbb{R}^n$ is the i th unit vector, $\boldsymbol{\varepsilon} = \nabla_{\text{sym}} \mathbf{u} := \frac{1}{2}(\nabla \mathbf{u} + \nabla \mathbf{u}^T) \in \mathbb{R}_{\text{sym}}^{d \times d}$ is the linearized strain tensor, \mathbb{C}_i is the fourth-order elasticity tensor for phase i , α_i is a temperature-dependent term that defines each “well-height”, and $\boldsymbol{\varepsilon}_i$ denotes the transformation strain of phase i . It has been argued by Ball and James (1987, 1992) that the microscopic energy density of such a material can be defined in terms of the individual phase energy densities in the following fashion:

$$W(\boldsymbol{\varepsilon}) = \min_{i=1, \dots, n} [W(\boldsymbol{\varepsilon}, \mathbf{e}_i)]. \quad (1)$$

The essential concept being advanced is that at each point in the body, the material will convert to the phase that will generate the lowest local energy. This, in turn, generates what can appropriately be termed a process of equilibrium (reversible) phase transformation. If one considers the minimization of the potential energy of a body under Dirichlet boundary conditions, then one is faced with the problem of minimizing the integral of the energy density (1) over the body of interest. This integral is a functional of the deformation and is well known not to be weakly lower semi-continuous (wlsc). Lack of the wlsc property implies non-existence of a minimizing deformation for given boundary data and hence indicates the formation of microstructure; see e.g. Ball and James (1987, 1992). This primary difficulty can be elegantly circumvented by utilizing the quasi-convex relaxation of the energy density (1) in the integrand of the total potential energy of the body (Kohn, 1991; Smyshlyaev and Willis, 1998; Dacorogna, 1989). The result of this procedure is a potential energy functional that is wlsc. With wlsc and the addition of a mild coercivity condition on the functional, one has a well-established existence theorem for minimizing deformations (Dacorogna, 1989). We may call such deformations macroscopic as micro- and mesoscopic structure is averaged out. Nevertheless, analyzing the macroscopic deformation gradients and the way the quasi-convex hull is formed a good prediction of various aspects of fine structure in martensitic alloys can be given—including for example observed twin structures, habit planes, etc. (Ball and James, 1987, 1992; Bhattacharya, 1993a,b; Bhattacharya and Kohn, 1995, 1996; Bhattacharya et al., 1997; Bhattacharya and James, 1999; Shield, 1995; Khachaturyna, 1983). Interesting applications in dislocation theory have also recently appeared (Ortiz et al., 2000).

The aforementioned procedure is now well established in the mathematical literature concerning non-convex analysis and it has been applied successfully to the notions of phase transformation. One “detraction”, however, of this procedure is that it generates an equilibrium model of phase transformation. Thus the model generated is incapable of predicting progressive evolution in homogeneous states of deformation and hysteresis effects—both of which are often of great interest. Some macroscopic models that attempt to describe phase transformation in an evolutionary manner with hysteresis

often employ as an internal variable the phase fractions $\mathbf{c} \in \mathcal{P}^n = \text{conv}(\mathcal{P}_{\text{pure}}^n)$ where $\mathcal{P}_{\text{pure}}^n = \{\mathbf{e}_1, \dots, \mathbf{e}_n\}$; see e.g. Carstensen and Plecháč (2001), Govindjee and Miehe (2001), Kuczma et al. (1999), Mielke and Theil (1999), Hall and Govindjee (1999), Levitas (1998), Mielke et al. (1998), Huang and Brinson (1998), Boyd and Lagoudas (1996), and Müller and Xu (1991). Geometrically, \mathcal{P}^n is a convex polytope whose extremal points are given by $\mathcal{P}_{\text{pure}}^n$. An alternative method using gradient Young measures is provided in Roubicek (2001).

In this paper, we do not directly address the evolutionary problem, rather we consider in some detail the free energy density of the phase transforming material as parameterized by the phase fractions. In particular, we adopt the highly successful formalism of quasi-convex analysis to describe a mathematically well-motivated free energy density $QW(\boldsymbol{\varepsilon}, \mathbf{c})$ which is defined in Eq. (5). This function is derived mathematically solely from the functions $W(\cdot, \mathbf{e}_i)$, $i = 1, \dots, n$, using the notion of quasi-convex relaxation at fixed volume fraction. Hence, $QW(\boldsymbol{\varepsilon}, \mathbf{c})$ is given as the minimal energy in a representative volume element where the minimization is done over all possible mesoscopic arrangements of the phases which are compatible with a given volume fraction $\mathbf{c} \in \mathcal{P}^n$ and all mesoscopic deformations with macroscopic strain $\boldsymbol{\varepsilon}$; see e.g. Avellaneda and Milton (1989) or Smyshlyaev and Willis (1998). The relevance of $QW(\boldsymbol{\varepsilon}, \mathbf{c})$ for the modeling of the rate-independent evolution of microstructure was first emphasized in Mielke et al. (1998) and Mielke and Theil (1999) and further investigated in Mielke et al. (2002) where a mathematical existence theorem for the two-phase situation is given. For a numerical investigation see Carstensen and Plecháč (2001).

The mathematical justification of the up-scaling from the micro- to the macroscale is addressed in Theil (2002) and Mielke (2002). We also remark here that many of the general theorems, propositions, and lemmas presented here can in fact be inferred or directly found in Kohn (1991) and Smyshlyaev and Willis (1998). Our intended contribution is a more compact and manageable presentation of these results from our own perspective which then allows for additional insights and applications that follow. For a more mathematical comparison between the different bounds we refer to Firoozye (1991) and Smyshlyaev and Willis (1998) and the references given therein.

If the elasticity tensors are assumed to be identical (i.e., $\mathbb{C}_i = \mathbb{C}$), then one can make considerable progress and the macroscopic free energy density takes the form

$$QW(\boldsymbol{\varepsilon}, \mathbf{c}) = \sum_{i=1}^n c_i W(\boldsymbol{\varepsilon}, \mathbf{e}_i) + w_{\text{mix}}(\mathbf{c}), \quad \mathbf{c} = (c_1, \dots, c_n)^T,$$

where the summation term corresponds to the Taylor upper bound and the free energy of mixing $w_{\text{mix}}: \mathcal{P}^n \rightarrow (-\infty, 0]$ is convex and satisfies $w_{\text{mix}}(\mathbf{e}_i) = 0$. While $w_{\text{mix}}(\theta \mathbf{e}_i + (1 - \theta) \mathbf{e}_j)$ can be given explicitly for $\theta \in [0, 1]$ and all $i \neq j$ (see Kohn, 1991), it is not known how to compute $w_{\text{mix}}(\mathbf{c})$ in the general case; for a discussion see e.g. Smyshlyaev and Willis (1998) for $n = 3$ and Mielke (2000) for general n . Here we provide upper and lower estimates w^{upp} and w^{low} for $w_{\text{mix}}(\mathbf{c})$ in terms of the function $\psi: \mathbb{R}_*^n = \{\boldsymbol{\eta} \in \mathbb{R}^n \mid \boldsymbol{\eta} \cdot \mathbf{e}_* = \sum \eta_j = 0\} \rightarrow \mathbb{R}$ given by

$$\psi(\boldsymbol{\eta}) = \min\left\{-\frac{1}{2}[\boldsymbol{\omega} \cdot \mathbb{C} : \boldsymbol{\varepsilon}^{\boldsymbol{\eta}}] \cdot \mathbf{T}^{-1}[\boldsymbol{\omega} \cdot \mathbb{C} : \boldsymbol{\varepsilon}^{\boldsymbol{\eta}}] \mid \boldsymbol{\omega} \in \mathbb{S}^{d-1}\right\} \leq 0 \quad (2)$$

with

$$\boldsymbol{\varepsilon}^\eta = \sum_{j=1}^n \eta_j \boldsymbol{\varepsilon}_j,$$

where $\mathbf{e}_* = (1, \dots, 1)^T \in \mathbb{R}^n$, $\mathbf{T}(\boldsymbol{\omega})$ is the acoustic tensor, and \mathbb{S}^{d-1} is the unit sphere embedded in \mathbb{R}^d . With $\mathbf{M}(\mathbf{c}) = \text{diag}(\mathbf{c}) - \mathbf{c} \otimes \mathbf{c}$ and $m = (n^2 - n)/2$ one obtains the lower bound

$$w^{\text{low}}(\mathbf{c}) = \min \left\{ \sum_{j=1}^m \psi(\boldsymbol{\eta}_j) \mid \boldsymbol{\eta}_j \in \mathbb{R}_*^n, \sum_{j=1}^m \boldsymbol{\eta}_j \otimes \boldsymbol{\eta}_j = \mathbf{M}(\mathbf{c}) \right\}. \tag{3}$$

By lamination theory, an upper bound is every function $w^{\text{upp}} : \mathcal{P}^n \rightarrow \mathbb{R}$ satisfying $w^{\text{upp}}(\mathbf{e}_i) \geq 0$ and

$$w^{\text{upp}}(\theta \mathbf{c}^{(1)} + (1 - \theta) \mathbf{c}^{(2)}) \geq \theta w^{\text{upp}}(\mathbf{c}^{(1)}) + (1 - \theta) w^{\text{upp}}(\mathbf{c}^{(2)}) + \theta(1 - \theta) \psi(\mathbf{c}^{(1)} - \mathbf{c}^{(2)})$$

for any two $\mathbf{c}^{(1)}, \mathbf{c}^{(2)} \in \mathcal{P}^n$, $\theta \in [0, 1]$. We also note that this result can be applied recursively for iterative improvement of the bound (Kohn, 1991; Smyshlyaev and Willis, 1998; Goldsztein, 2001).

The theory for computing the bounds mentioned above uses \mathbb{H} -measures for minimizing sequences of optimal arrangements of the phase mixture as was proposed in Kohn (1991) and Smyshlyaev and Willis (1998). The lower estimate is obtained by relaxing the set of \mathbb{H} -measures whereas the upper estimate relies on the mixing formula for laminated \mathbb{H} -measures. Since these are only bounds, there is interest in estimating their preciseness. To this end we pursue two avenues in this paper: (1) we examine some special cases analytically to find subsets of \mathcal{P}^n where some of the bounds are exact and (2) we consider the numerical computation of the bounds for the 4-variant case. With respect to analytical results, we are able to show that the function $w_{\text{mix}} : \mathcal{P}^n \rightarrow \mathbb{R}$ takes the so-called Reu\ss form

$$w_{\text{mix}}(\mathbf{c}) = w_{\text{Reu\ss}}(\mathbf{c}) = -\frac{1}{2} \sum_{j=1}^n c_j \boldsymbol{\varepsilon}_j : \mathbb{C} : \boldsymbol{\varepsilon}_j + \frac{1}{2} \sum_{j=1}^n \sum_{k=1}^n c_j c_k \boldsymbol{\varepsilon}_j : \mathbb{C} : \boldsymbol{\varepsilon}_k$$

whenever $\mathbf{c} \in \mathcal{P}^n$ can be expressed as $\mathbf{c} = \theta \mathbf{c}^{(1)} + (1 - \theta) \mathbf{c}^{(2)}$ with $\theta \in (0, 1)$. The points $\mathbf{c}^{(l)}$ satisfy $w_{\text{mix}}(\mathbf{c}^{(l)}) = w_{\text{Reu\ss}}(\mathbf{c}^{(l)})$ for $l \in \{1, 2\}$ and their associated averaged transformation strains are symmetrically rank-one connected (compatible); that is $\boldsymbol{\varepsilon}^\eta = \mathbf{a} \otimes_{\text{sym}} \mathbf{b}$ for some $\mathbf{a}, \mathbf{b} \in \mathbb{R}^d$ where $\boldsymbol{\eta} = \mathbf{c}^{(2)} - \mathbf{c}^{(1)}$ and $\mathbf{a} \otimes_{\text{sym}} \mathbf{b} = \frac{1}{2}(\mathbf{a} \otimes \mathbf{b} + \mathbf{b} \otimes \mathbf{a})$; see Corollary 5.4. The importance of this result emanates from the fact that the set of such phase fractions is rather large. Thus, we have a closed form approximation for the free energy of mixing in the n -variant case. An assessment of the accuracy of the Reu\ss bound is made by computing in the 4-variant case an upper bound and an improved lower bound utilizing a relaxation of the set of \mathbb{H} -measures. We observe from this exercise that the Reu\ss bound provides a computationally useful approximation to the actual mixing energy. The predictive power of using this bound in evolutionary models has been demonstrated in Govindjee and Miehe (2001) and Hall and Govindjee (2002) through comparison to

the single crystal experiments of Shield (1995). Here we present an illustrative example employing the evolutionary model in Hall and Govindjee (2002).

2. Quasi-convex relaxation at fixed volume fraction

As a point of departure consider n stored-energy densities $W(\mathbf{F}, \mathbf{e}_j)$, $j = 1, \dots, n$, which are assumed to be quasi-convex in their first argument, where \mathbf{F} is the deformation gradient. An appropriate stored-energy density of the material is then given as

$$W(\mathbf{F}) = \min_{i=1, \dots, n} [W(\mathbf{F}, \mathbf{e}_i)]. \tag{4}$$

As noted in the introduction, this energy density is not quasi-convex and thus does not lead to a wsc potential energy. By relaxing this energy density we can recover the essential property of wsc. The appropriate relaxation in this case is a quasi-convex relaxation which for given volume fraction $\mathbf{c} \in \mathcal{P}^n$ is defined via

$$QW(\mathbf{F}, \mathbf{c}) = \inf \left\{ \int_{Q^d} W(\mathbf{F} + \nabla \boldsymbol{\varphi}(\mathbf{y}), \boldsymbol{\chi}(\mathbf{y})) \, d\mathbf{y} \mid \boldsymbol{\varphi} \in W_{\text{per}}^{1,p}(Q^d), \right. \\ \left. \boldsymbol{\chi}(\mathbf{y}) \in \mathcal{P}_{\text{pure}}^n, \int_{Q^d} \boldsymbol{\chi}(\mathbf{y}) \, d\mathbf{y} = \mathbf{c} \right\}, \tag{5}$$

where $Q^d = (0, 1)^d \subset \mathbb{R}^d$. It can be shown (cf. Mielke et al., 1998) that for each $\mathbf{c} \in \mathcal{P}^n$ the function $\mathbf{F} \mapsto QW(\mathbf{F}, \mathbf{c})$ is quasi-convex and for each \mathbf{F} the function $\mathbf{c} \mapsto QW(\mathbf{F}, \mathbf{c})$ is convex. Moreover, the quasi-convex hull QW of the function W in Eq. (4) is given by $QW(\mathbf{F}) = \min_{\mathbf{c} \in \mathcal{P}^n} QW(\mathbf{F}, \mathbf{c})$; see Kohn (1991).

In this work we completely restrict our attention to the case of linearized elasticity where additionally each phase has the same elastic tensor \mathbb{C} :

$$W(\mathbf{F}, \mathbf{e}_i) \approx W(\boldsymbol{\varepsilon}, \mathbf{e}_i) = \frac{1}{2}(\boldsymbol{\varepsilon} - \boldsymbol{\varepsilon}_i) : \mathbb{C} : (\boldsymbol{\varepsilon} - \boldsymbol{\varepsilon}_i) + \alpha_i. \tag{6}$$

As mentioned above $\boldsymbol{\varepsilon} = \nabla_{\text{sym}} \mathbf{u}$ is the linearized strain, $\boldsymbol{\varepsilon}_i$ are the transformation strains, and α_i are the heights of the wells which usually depend on the temperature which is assumed to be constant here.

Proposition 2.1. *If all $W(\mathbf{F}, \mathbf{e}_j)$, $j = 1, \dots, n$, have form (6) then the relaxed energy density takes the form $QW(\boldsymbol{\varepsilon}, \mathbf{c}) = \sum_{j=1}^n c_j W(\boldsymbol{\varepsilon}, \mathbf{e}_j) + w_{\text{mix}}(\mathbf{c})$, where the mixture term $w_{\text{mix}} : \mathcal{P}^n \rightarrow \mathbb{R}$ is convex and is given by*

$$w_{\text{mix}}(\mathbf{c}) = \inf \left\{ \int_{Q^d} \nabla_{\text{sym}} \boldsymbol{\varphi} : \mathbb{C} : \left(\frac{1}{2} \nabla_{\text{sym}} \boldsymbol{\varphi} - \sum_{j=1}^n \chi_j(\mathbf{y}) \boldsymbol{\varepsilon}_j \right) \, d\mathbf{y} \mid \right. \\ \left. \int_{Q^d} \boldsymbol{\chi}(\mathbf{y}) \, d\mathbf{y} = \mathbf{c}, \boldsymbol{\chi}(\mathbf{y}) \in \mathcal{P}_{\text{pure}}^n, \boldsymbol{\varphi} \in W_{\text{per}}^{1,2}(Q^d) \right\}. \tag{7}$$

This form follows immediately using the quadratic structure of the energy density, $\int \nabla_{\text{sym}} \boldsymbol{\varphi} \, \text{d}\mathbf{y} = \mathbf{0}$, $\int \boldsymbol{\chi}(\mathbf{y}) \, \text{d}\mathbf{y} = \mathbf{c}$ and $\sum_{j=1}^n \chi_j(\mathbf{y}) \equiv 1$.

Since $\boldsymbol{\varphi}$ appears quadratically in $w_{\text{mix}}(\mathbf{c})$ we may eliminate it by first minimizing with respect to $\boldsymbol{\varphi}$ and keeping the phase indicator field $\boldsymbol{\chi}$ fixed. This is done most easily using Fourier series

$$\boldsymbol{\varphi}(\mathbf{y}) = \sum_{\boldsymbol{\xi} \in \Gamma_*} \boldsymbol{\varphi}_{\boldsymbol{\xi}} e^{i\boldsymbol{\xi} \cdot \mathbf{y}}, \quad \boldsymbol{\chi}(\mathbf{y}) = \sum_{\boldsymbol{\xi} \in \Gamma} \chi_{\boldsymbol{\xi}} e^{i\boldsymbol{\xi} \cdot \mathbf{y}}, \quad \boldsymbol{\chi}_0 = \mathbf{c},$$

where $\Gamma = (2\pi\mathbb{Z})^d$ and $\Gamma_* = \Gamma \setminus \{\mathbf{0}\}$. Inserting this form into $w_{\text{mix}}(\mathbf{c})$ we find a decoupling between different $\boldsymbol{\xi}$'s. Thus the Fourier coefficient $\boldsymbol{\varphi}_{\boldsymbol{\xi}} = \bar{\boldsymbol{\varphi}}_{-\boldsymbol{\xi}} \in \mathbb{C}^d$ can be found by minimizing the following term with respect to $\boldsymbol{\varphi}_{\boldsymbol{\xi}}$

$$\frac{1}{2} [i\boldsymbol{\xi} \otimes_{\text{sym}} \boldsymbol{\varphi}_{\boldsymbol{\xi}}] : \mathbb{C} : [i\boldsymbol{\xi} \otimes_{\text{sym}} \boldsymbol{\varphi}_{\boldsymbol{\xi}}] - \text{Re} \left\{ [i\boldsymbol{\xi} \otimes_{\text{sym}} \boldsymbol{\varphi}_{\boldsymbol{\xi}}] : \mathbb{C} : \left[\sum_{j=1}^n (\chi_{\boldsymbol{\xi}})_j \boldsymbol{\varepsilon}_j \right] \right\}. \quad (8)$$

After some elementary calculations we arrive at

$$w_{\text{mix}}(\mathbf{c}) = \inf \left\{ I(\boldsymbol{\chi}) \mid \int_{Q^d} \boldsymbol{\chi}(\mathbf{y}) \, \text{d}\mathbf{y} = \mathbf{c}, \boldsymbol{\chi}(\mathbf{y}) \in \mathcal{P}_{\text{pure}}^n \right\}$$

with

$$I(\boldsymbol{\chi}) = -\frac{1}{2} \sum_{\boldsymbol{\xi} \in \Gamma_*} \left(\boldsymbol{\xi} \cdot \mathbb{C} : \left[\sum_{j=1}^n (\chi_{\boldsymbol{\xi}})_j \boldsymbol{\varepsilon}_j \right] \right) \cdot \mathbf{T}(\boldsymbol{\xi})^{-1} \left(\boldsymbol{\xi} \cdot \mathbb{C} : \left[\sum_{j=1}^n (\chi_{\boldsymbol{\xi}})_j \boldsymbol{\varepsilon}_j \right] \right).$$

Here the acoustic tensor $\mathbf{T}(\boldsymbol{\xi})$ is defined via $\mathbf{u} \cdot \mathbf{T}(\boldsymbol{\xi}) \mathbf{u} = [\boldsymbol{\xi} \otimes_{\text{sym}} \mathbf{u}] : \mathbb{C} : [\boldsymbol{\xi} \otimes_{\text{sym}} \mathbf{u}]$ and thus is homogeneous of degree 2 in $\boldsymbol{\xi} \in \mathbb{R}^d$. Introducing $\mathbf{G}(\boldsymbol{\xi}) \in \mathbb{R}_{\text{sym}}^{n \times n}$ via

$$G(\boldsymbol{\xi})_{jk} = \frac{1}{2} (\boldsymbol{\xi} \cdot \mathbb{C} : \boldsymbol{\varepsilon}_j) \cdot \mathbf{T}(\boldsymbol{\xi})^{-1} (\boldsymbol{\xi} \cdot \mathbb{C} : \boldsymbol{\varepsilon}_k), \quad (9)$$

we obtain the compact formula

$$I(\boldsymbol{\chi}) = - \sum_{\boldsymbol{\xi} \in \Gamma_*} \mathbf{G}(\boldsymbol{\xi}) : (\bar{\boldsymbol{\chi}}_{\boldsymbol{\xi}} \otimes \boldsymbol{\chi}_{\boldsymbol{\xi}}).$$

The computation of w_{mix} from this form of $I(\boldsymbol{\chi})$ is non-trivial due to the complicated character of the optimization constraints associated with the Fourier transform of the microstructure indicator field $\boldsymbol{\chi}$. In the next section, we review the notion of \mathbb{H} -measures to re-characterize this problem and discuss two useful means of approaching w_{mix} in an approximate sense.

3. The \mathbb{H} -measure associated with the microstructure $\boldsymbol{\chi}$

The function $\boldsymbol{\chi} : Q^d \rightarrow \mathcal{P}_{\text{pure}}^n$ defines a microstructure of pure phases having the volume average $\mathbf{c} = \int_{Q^d} \boldsymbol{\chi}(\mathbf{y}) \, \text{d}\mathbf{y}$. We associate to each function $\boldsymbol{\chi}$ a matrix-valued measure

$\boldsymbol{\mu} = \tilde{\boldsymbol{\mu}}(\boldsymbol{\chi})$ on the unit sphere \mathbb{S}^{d-1} . The values of $\boldsymbol{\mu}$ will lie in the set $\mathbb{H}_{\geq 0}^n$ of positive semidefinite Hermitian matrices in $\mathbb{C}^{n \times n}$. For any measurable $\Sigma \subset \mathbb{S}^{d-1}$ we let

$$\boldsymbol{\mu}(\Sigma) = \sum_{\xi \in \Gamma^*, \xi/|\xi| \in \Sigma} \boldsymbol{\chi}_\xi \otimes \bar{\boldsymbol{\chi}}_\xi \in \mathbb{H}_{\geq 0}^n.$$

The measure is a homogeneous \mathbb{H} -measure in the sense of Tartar (1990) when the generating sequence $\mathbf{u}^{(n)}(\mathbf{y}) = \boldsymbol{\chi}(n\mathbf{y}) - \mathbf{c}$ is considered.

Introducing the linear functional

$$J : \text{meas}(\mathbb{S}^{d-1}, \mathbb{H}_{\geq 0}^n) \rightarrow \mathbb{R},$$

$$\boldsymbol{\mu} \mapsto J(\boldsymbol{\mu}) = - \int_{\omega \in \mathbb{S}^{d-1}} \mathbf{G}(\omega) : \boldsymbol{\mu}(d\omega), \tag{10}$$

we obtain the relation $I(\boldsymbol{\chi}) = J(\hat{\boldsymbol{\mu}}(\boldsymbol{\chi}))$, where $\hat{\boldsymbol{\mu}}(\boldsymbol{\chi}) = \text{Re } \tilde{\boldsymbol{\mu}}(\boldsymbol{\chi})$. This follows from the symmetry $\mathbf{G}(-\omega) = \mathbf{G}(\omega)$ which tells us that J depends only on the real part of $\boldsymbol{\mu}$. We formally define $\hat{\boldsymbol{\mu}}(\cdot)$ as

$$\hat{\boldsymbol{\mu}} : L^\infty(Q^d, \mathcal{P}_{\text{pure}}^n) \rightarrow \text{meas}(\mathbb{S}^{d-1}, \mathbb{P}^n),$$

$$\boldsymbol{\chi} \mapsto \hat{\boldsymbol{\mu}}(\boldsymbol{\chi}) = \text{Re } \tilde{\boldsymbol{\mu}}(\boldsymbol{\chi}),$$

where $\mathbb{P}^n = \{\mathbf{B} \in \mathbb{R}^{n \times n} \mid \mathbf{B} = \mathbf{B}^T, \mathbf{B} \text{ positive semidefinite}\}$. It then follows that each $\boldsymbol{\mu} = \hat{\boldsymbol{\mu}}(\boldsymbol{\chi})$ satisfies

- (i) $\boldsymbol{\mu}(\Sigma)\mathbf{e}_* = \mathbf{0}$ for all $\Sigma \subset \mathbb{S}^{d-1}$,
 - (ii) $\boldsymbol{\mu}(\mathbb{S}^{d-1}) = \mathbf{M}(\mathbf{c})$ where $\mathbf{c} = \int \boldsymbol{\chi}(\mathbf{y}) d\mathbf{y}$,
 - (iii) $\boldsymbol{\mu}(-\Sigma) = \boldsymbol{\mu}(\Sigma) \in \mathbb{P}^n$ for all $\Sigma \subset \mathbb{S}^{d-1}$,
- (11)

where $\mathbf{M}(\mathbf{c})$ is as defined right before Eq. (3). For each $\mathbf{c} \in \mathcal{P}^n$ we define the subsets of matrix-valued measures

$$\mathcal{H}(\mathbf{c}) = \text{closure} \left\{ \hat{\boldsymbol{\mu}}(\boldsymbol{\chi}) \mid \int_{Q^d} \boldsymbol{\chi}(\mathbf{y}) d\mathbf{y} = \mathbf{c} \right\},$$

$$\overline{\mathcal{H}}(\mathbf{c}) = \{ \boldsymbol{\mu} \in \text{meas}(\mathbb{S}^{d-1}, \mathbb{P}^n) \mid \text{Eq. (11) holds} \}.$$

Clearly, $\mathcal{H}(\mathbf{c}) \subset \overline{\mathcal{H}}(\mathbf{c})$ and $\overline{\mathcal{H}}(\mathbf{c})$ is convex. The function w_{mix} can now be expressed as

$$w_{\text{mix}}(\mathbf{c}) = \inf \{ J(\boldsymbol{\mu}) \mid \boldsymbol{\mu} \in \mathcal{H}(\mathbf{c}) \}. \tag{12}$$

The difficulty in calculating $w_{\text{mix}}(\mathbf{c})$ is the same as in calculating $\mathcal{H}(\mathbf{c})$. There are at present no good characterizations of $\mathcal{H}(\mathbf{c})$. To make progress one is faced with a situation where only bounds can be computed. Constructing \mathcal{H}^{inn} and \mathcal{H}^{out} with $\mathcal{H}^{\text{inn}}(\mathbf{c}) \subset \mathcal{H}(\mathbf{c}) \subset \mathcal{H}^{\text{out}}(\mathbf{c})$, we obtain upper and lower bounds for w_{mix} if $\mathcal{H}(\mathbf{c})$ in infimum (12) is replaced by $\mathcal{H}^{\text{inn}}(\mathbf{c})$ and $\mathcal{H}^{\text{out}}(\mathbf{c})$, respectively. In Section 4 the lamination mixture formula for \mathbb{H} -measures (see Theorem 4.1) is employed to find upper bounds. In Section 5.1 we will use $\mathcal{H}^{\text{out}} = \overline{\mathcal{H}}(\mathbf{c})$ to obtain a lower bound.

4. Upper bounds

Since w_{mix} is non-positive we have the trivial bound $w_{\text{mix}}(c) \leq 0$; to improve this bound we need to find a suitable inner approximation of $\mathcal{H}(\mathbf{c})$. In fact, in the light of the Krein–Milman theorem, it is sufficient to characterize (or approximate) only extremal points of such a subset.

There is no general theory to describe $\mathcal{H}(\mathbf{c})$ suitably, however the *lamination mixture formula*, which is due to Avellaneda and Milton (1989), Tartar (1990) and Kohn (1991) allows us to construct new \mathbb{H} -measures as mixtures of two given ones.

Theorem 4.1. *Assume $\boldsymbol{\mu}^{(1)} \in \mathcal{H}(\mathbf{c}^{(1)})$, $\boldsymbol{\mu}^{(2)} \in \mathcal{H}(\mathbf{c}^{(2)})$, $\theta \in [0, 1]$ and $\boldsymbol{\omega} \in \mathbb{S}^{d-1}$, then there exists a $\boldsymbol{\mu} \in \mathcal{H}(\theta\mathbf{c}^{(1)} + (1 - \theta)\mathbf{c}^{(2)})$ of the form*

$$\boldsymbol{\mu} = \theta\boldsymbol{\mu}^{(1)} + (1 - \theta)\boldsymbol{\mu}^{(2)} + \theta(1 - \theta)(\mathbf{c}^{(2)} - \mathbf{c}^{(1)}) \otimes (\mathbf{c}^{(2)} - \mathbf{c}^{(1)})\hat{\boldsymbol{\delta}}_{\boldsymbol{\omega}}, \tag{13}$$

where $\hat{\boldsymbol{\delta}}_{\boldsymbol{\omega}} = \frac{1}{2}(\boldsymbol{\delta}_{\boldsymbol{\omega}} + \boldsymbol{\delta}_{-\boldsymbol{\omega}})$ and $\boldsymbol{\delta}_{\boldsymbol{\omega}} \in \text{meas}(\mathbb{S}^{d-1}, [0, 1])$ is the Dirac measure located at $\boldsymbol{\omega} \in \mathbb{S}^{d-1}$.

Note that the statement in Eq. (13) is consistent with

$$\begin{aligned} \mathbf{M}(\theta\mathbf{c}^{(1)} + (1 - \theta)\mathbf{c}^{(2)}) &= \theta\mathbf{M}(\mathbf{c}^{(1)}) + (1 - \theta)\mathbf{M}(\mathbf{c}^{(2)}) \\ &\quad + \theta(1 - \theta)(\mathbf{c}^{(2)} - \mathbf{c}^{(1)}) \otimes (\mathbf{c}^{(2)} - \mathbf{c}^{(1)}). \end{aligned} \tag{14}$$

This theorem implies convexity of $\mathcal{H}(\mathbf{c})$, since mixing with $\mathbf{c}^{(1)} = \mathbf{c}^{(2)} = \mathbf{c}$ does not generate an additional quadratic term. Another immediate consequence is the estimate

$$\begin{aligned} w_{\text{mix}}(\theta\mathbf{c}^{(1)} + (1 - \theta)\mathbf{c}^{(2)}) &\leq \theta w_{\text{mix}}(\mathbf{c}^{(1)}) + (1 - \theta)w_{\text{mix}}(\mathbf{c}^{(2)}) \\ &\quad + \theta(1 - \theta)\psi(\mathbf{c}^{(1)} - \mathbf{c}^{(2)}), \end{aligned} \tag{15}$$

where $\theta \in [0, 1]$ and $\psi : \mathbb{R}^n \rightarrow \mathbb{R}$ is given as

$$\psi(\boldsymbol{\eta}) = \min\{-\mathbf{G}(\boldsymbol{\omega}) : (\boldsymbol{\eta} \otimes \boldsymbol{\eta}) \mid \boldsymbol{\omega} \in \mathbb{S}^{d-1}\}, \tag{16}$$

where $\mathbf{G}(\boldsymbol{\omega})$ is defined in Eq. (9). Note this expression is fully compatible with the relation given in Section 1 in Eq. (2) and is also known as the rank-one convexification (bound).

To see the validity of Eq. (15) choose $\boldsymbol{\mu}^{(j)} \in \mathcal{H}(\mathbf{c}^{(j)})$ with $w_{\text{mix}}(\mathbf{c}^{(j)}) = J(\boldsymbol{\mu}^{(j)})$ for $j = 1$ and 2. Further choose $\boldsymbol{\omega} \in \mathbb{S}^{d-1}$ such that $\psi(\mathbf{c}^{(1)} - \mathbf{c}^{(2)}) = -\mathbf{G}(\boldsymbol{\omega}) : [(\mathbf{c}^{(1)} - \mathbf{c}^{(2)}) \otimes (\mathbf{c}^{(1)} - \mathbf{c}^{(2)})]$. Then, the measure $\boldsymbol{\mu}$ as defined in Eq. (13) lies in $\mathcal{H}(\theta\mathbf{c}^{(1)} + (1 - \theta)\mathbf{c}^{(2)})$ and Eq. (12) gives Eq. (15). As $\psi(\boldsymbol{\eta}) \leq 0$, this implies better bounds than simple convexity in most cases. Starting with $\mathbf{0} \in \mathcal{H}(\mathbf{e}_j)$ we may inductively apply this formula to obtain non-trivial bounds.

It was first observed in Kohn (1991), where the theory given in Section 3 was actually developed, that this approach gives an exact expression for w_{mix} in the case of two phases, viz.,

$$w_{\text{mix}}(\theta\mathbf{e}_j + (1 - \theta)\mathbf{e}_k) = \theta(1 - \theta)\psi(\mathbf{e}_j - \mathbf{e}_k). \tag{17}$$

This result follows immediately since the lower and upper bounds for $w_{\text{mix}}(\mathbf{c})$ coincide. Our Theorem 6.2 generalizes this fact to the case of n phases, if all transformation strains lie on a single straight line. In general, however, we only obtain upper bounds.

Proposition 4.2. For $\mathbf{c} \in \mathcal{P}^n$ define $\mathbf{c}^{(k)} = (c_1 + \dots + c_k)^{-1}(c_1 \mathbf{e}_1 + \dots + c_k \mathbf{e}_k)$, then

$$w_{\text{mix}}(\mathbf{c}) \leq \sum_{j=2}^n \frac{(c_1 + \dots + c_{j-1})c_j}{c_1 + \dots + c_j} \psi(\mathbf{c}^{(j-1)} - \mathbf{e}_j). \tag{18}$$

By permutation of the points $\mathbf{e}_1, \dots, \mathbf{e}_n$ we can generate other upper bounds.

Proof. We proceed by induction. Obviously, the result is true for $\mathbf{c} = \mathbf{c}^{(1)} = \mathbf{e}_1$. Now, assume it is true for $\mathbf{c}^{(k)} \in \text{conv}\{\mathbf{e}_1, \dots, \mathbf{e}_k\}$ with $1 \leq k < n$. Then, for $\mathbf{c}^{(k+1)}$ we have the formula

$$\mathbf{c}^{(k+1)} = \frac{c_1 + \dots + c_k}{c_1 + \dots + c_{k+1}} \mathbf{c}^{(k)} + \frac{c_{k+1}}{c_1 + \dots + c_{k+1}} \mathbf{e}_{k+1}.$$

Applying Eq. (15) with $\mathbf{c}^{(1)} = \mathbf{c}^{(k)}$ and $\mathbf{c}^{(2)} = \mathbf{e}_{k+1}$ the result follows using $w_{\text{mix}}(\mathbf{e}_{k+1}) = 0$. □

Of course, the upper bound in the right-hand side of Eq. (18) may be further reduced by applying Eq. (15) again. In fact, in typical cases it needs infinitely many applications of the lamination formula to approach the lowest level. This corresponds to infinite sequential lamination; see Smyshlyaev and Willis (1998).

In principle, the definition $w^{\text{upp}}(\mathbf{c}) = \max\{\tilde{w}(\mathbf{c}) \mid \tilde{w} \text{ satisfies Eq. (15), } \tilde{w}(\mathbf{e}_j) \leq 0, j = 1, \dots, n\}$ defines the best upper bound for $w_{\text{mix}}(\mathbf{c})$ which can be obtained from lamination. For practical purposes it is better to write w^{upp} as a minimum, since then each candidate \tilde{w} provides a true upper bound

$$w^{\text{upp}}(\mathbf{c}) = \min\{\tilde{w}(\mathbf{c}) \mid \tilde{w} \text{ satisfies Eq. (19), } \tilde{w}(\mathbf{e}_j) \geq 0 \text{ for } j = 1, \dots, n\},$$

where now the condition reads

$$\tilde{w}(\theta \mathbf{c}^{(1)} + (1 - \theta) \mathbf{c}^{(2)}) \geq \theta \tilde{w}(\mathbf{c}^{(1)}) + (1 - \theta) \tilde{w}(\mathbf{c}^{(2)}) + \theta(1 - \theta) \psi(\mathbf{c}^{(1)} - \mathbf{c}^{(2)}). \tag{19}$$

In Section 6 we will utilize this lamination bound to compute the mixing energy for a 4-variant material and compare it to the lower bounds to be discussed next. The application of a less general albeit similar bound has been made in the case of martensitic phase transformations by Goldsztein (2001) when the transformation strains are purely deviatoric.

5. Lower bounds

In this section we consider two lower bounds to the mixing energy. First we construct a lower bound by looking at a particular outer approximation to $\mathcal{H}(\mathbf{c})$. Second we consider a further relaxation of the problem by constructing a lower bound directly from the quasi-convex relaxation process by ignoring the issue of compatibility. It will

be seen that this bound directly corresponds to the notion of a stress ensemble and thus this second lower bound is termed a Reuß bound. The corresponding Taylor bound which is obtained by assuming constant strain leads to an uninteresting upper bound $w_{\text{mix}}(\mathbf{c}) \leq 0$, which follows trivially from $w_{\text{mix}}(\mathbf{e}_j) = 0$ and convexity.

5.1. \mathbb{H} -measure lower bound

To find a lower bound consider $\mathcal{H}(\mathbf{c}) \subset \overline{\mathcal{H}}(\mathbf{c})$ so that one may write

$$w_{\text{mix}}(\mathbf{c}) \geq w^{\text{low}}(\mathbf{c}) = \inf \left\{ - \int_{\mathbb{S}^{d-1}} \mathbf{G}(\boldsymbol{\omega}) : \boldsymbol{\mu}(d\boldsymbol{\omega}) \mid \boldsymbol{\mu} \in \overline{\mathcal{H}}(\mathbf{c}) \right\}.$$

It is possible to characterize $\overline{\mathcal{H}}(\mathbf{c})$ solely by algebraic conditions; thus it is easier to calculate $w^{\text{low}}(\mathbf{c})$ than $w_{\text{mix}}(\mathbf{c})$. In particular, following Smyshlyaev and Willis (1998) we will show that the calculation of $w^{\text{low}}(\mathbf{c})$ can be reduced to a finite dimensional minimization problem.

Since the mapping $J : \text{meas}(\mathbb{S}^{d-1}, \mathbb{H}_{\geq 0}^n) \rightarrow \mathbb{R}$ given in Eq. (10) is linear and since $\overline{\mathcal{H}}(\mathbf{c})$ is convex, closed and bounded, we can apply the Krein–Milman theorem which states that J attains its minimum on the extremal points of $\overline{\mathcal{H}}(\mathbf{c})$:

$$\text{ex}(\overline{\mathcal{H}}(\mathbf{c})) = \{ \boldsymbol{\mu} \in \overline{\mathcal{H}}(\mathbf{c}) \mid \overline{\mathcal{H}} \setminus \{ \boldsymbol{\mu} \} \text{ is convex} \}.$$

Recalling $m = (n^2 - n)/2$ and $\hat{\boldsymbol{\delta}}_{\boldsymbol{\omega}} = \frac{1}{2}(\boldsymbol{\delta}_{\boldsymbol{\omega}} + \boldsymbol{\delta}_{-\boldsymbol{\omega}}) \in \text{meas}(\mathbb{S}^{d-1}, [0, 1])$ this set can be characterized as follows.

Proposition 5.1. *We have $\boldsymbol{\mu} \in \text{ex}(\overline{\mathcal{H}}(\mathbf{c}))$ if and only if there exist directions $\boldsymbol{\omega}_1, \dots, \boldsymbol{\omega}_m \in \mathbb{S}^{d-1}$ and $\boldsymbol{\eta}_1, \dots, \boldsymbol{\eta}_m \in \mathbb{R}_*^n$ such that $\boldsymbol{\mu} = \sum_{j=1}^m \hat{\boldsymbol{\delta}}_{\boldsymbol{\omega}_j} \boldsymbol{\eta}_j \otimes \boldsymbol{\eta}_j$.*

Proof. We begin by showing that the support of $\boldsymbol{\mu}$ cannot be anything more than m discrete points. If it could, then it is always possible to find in \mathbb{S}^{d-1} , $m + 1$ pairwise disjoint symmetric Σ_j (i.e. $\Sigma_j = -\Sigma_j$) such that $\boldsymbol{\mu}(\Sigma_j) \neq 0$. Now, since all $\boldsymbol{\mu}(\Sigma_j)$ lie in the m -dimensional linear space $\{ \mathbf{M} \in \mathbb{R}_{\text{sym}}^{n \times n} \mid \mathbf{M} \mathbf{e}_* = \mathbf{0} \}$ the equation $\sum_{j=1}^{m+1} \alpha_j \boldsymbol{\mu}(\Sigma_j) = \mathbf{0}$ has a non-trivial solution $(\alpha_1, \dots, \alpha_{m+1}) \in \mathbb{R}^{m+1} \setminus \{ \mathbf{0} \}$. We may assume $|\alpha_j| \leq 1$ and define the two measures $\boldsymbol{\mu}^{\pm} \in \overline{\mathcal{H}}(\mathbf{c})$ via $\boldsymbol{\mu}^{\pm}(\Sigma) = (1 \pm \alpha_j) \boldsymbol{\mu}(\Sigma)$ if $\Sigma \subset \Sigma_j$ and $\boldsymbol{\mu}^{\pm}(\Sigma) = \boldsymbol{\mu}(\Sigma)$ if $\Sigma \cap \bigcup_{j=1}^{m+1} \Sigma_j = \emptyset$. Clearly, $\boldsymbol{\mu}^+ \neq \boldsymbol{\mu}^-$ and $\boldsymbol{\mu} = \frac{1}{2}(\boldsymbol{\mu}^+ + \boldsymbol{\mu}^-)$. Thus, $\boldsymbol{\mu}$ cannot be extremal, if there exist more than m pairwise disjoint sets with positive measure. This means that the measure must be concentrated on at most m points $\boldsymbol{\omega}_j$ (together with its antipode $-\boldsymbol{\omega}_j$). Hence, any extremal measure must take the form $\boldsymbol{\mu} = \sum_{j=1}^m \hat{\boldsymbol{\delta}}_{\boldsymbol{\omega}_j} \mathbf{M}_j$ with $\mathbf{M}_j \in \mathbb{P}_*^n = \{ \mathbf{M} \in \mathbb{P}^n \mid \mathbf{M} \mathbf{e}_* = \mathbf{0} \}$.

It remains to show that $\text{rank } \mathbf{M}_j \leq 1$. Each \mathbf{M}_j has the form $\mathbf{M}_j = \sum_{i=1}^{r_j} \boldsymbol{\eta}_{j,i} \otimes \boldsymbol{\eta}_{j,i}$ where $r_j = \text{rank } \mathbf{M}_j$ and $\boldsymbol{\eta}_{j,i} \neq \mathbf{0}$. To find a contradiction we assume $\sum_{j=1}^m r_j > m$, then as above $\sum_{j=1}^m \sum_{i=1}^{r_j} \alpha_{j,i} \boldsymbol{\eta}_{j,i} \otimes \boldsymbol{\eta}_{j,i} = \mathbf{0}$ has a non-trivial solution with $|\alpha_{j,i}| \leq 1$. The measures $\boldsymbol{\mu}^{\pm} = \sum_{j=1}^m \sum_{i=1}^{r_j} (1 \pm \alpha_{j,i}) \hat{\boldsymbol{\delta}}_{\boldsymbol{\omega}_j} \boldsymbol{\eta}_{j,i} \otimes \boldsymbol{\eta}_{j,i}$ are different, lie in $\overline{\mathcal{H}}(\mathbf{c})$ and satisfy $\boldsymbol{\mu} = \frac{1}{2}(\boldsymbol{\mu}^+ + \boldsymbol{\mu}^-)$. Thus, $\boldsymbol{\mu}$ cannot be an extremal measure which is the desired contradiction. \square

To formulate the main result of this section we recall the definition $\psi(\boldsymbol{\eta}) = \min\{-\mathbf{G}(\boldsymbol{\omega}) : (\boldsymbol{\eta} \otimes \boldsymbol{\eta}) | \boldsymbol{\omega} \in \mathbb{S}^{d-1}\}$ from Eq. (16). Moreover, introduce the sets $\mathbb{E}_*^n = \{\boldsymbol{\eta} \otimes \boldsymbol{\eta} \in \mathbb{P}_*^n \mid \boldsymbol{\eta} \in \mathbb{S}^{n-1}, \boldsymbol{\eta} \cdot \mathbf{e}_* = 0\}$ and $\mathbb{K}_*^n = \{\mathbf{M} \in \mathbb{P}_*^n \mid \text{tr}[\mathbf{M}] = 1\}$. Then $\mathbb{K}_*^n = \text{conv}(\mathbb{E}_*^n)$ and $\mathbb{E}_*^n = \text{ex}(\mathbb{K}_*^n)$. The set \mathbb{E}_*^n is a smooth manifold of dimension $(n - 2)$. The set \mathbb{K}_*^n lies in an affine subspace of $\mathbb{R}^{n \times n}$ of dimension $(n^2 - n)/2 - 1$ and has non-empty interior with respect to this subspace.

Finally, we define $\Psi : \mathbb{K}_*^n \rightarrow \mathbb{R}$ to be the largest convex function which satisfies $\Psi(\boldsymbol{\eta} \otimes \boldsymbol{\eta}) = \psi(\boldsymbol{\eta})$ for $\boldsymbol{\eta} \otimes \boldsymbol{\eta} \in \mathbb{E}_*^n$, viz.,

$$\Psi(\mathbf{M}) = \min \left\{ \sum_{j=1}^m \alpha_j \psi(\boldsymbol{\eta}_j) \mid \alpha_j \geq 0, \sum_{j=1}^m \alpha_j = 1, \boldsymbol{\eta}_j \otimes \boldsymbol{\eta}_j \in \mathbb{E}_*^n, \sum_{j=1}^m \alpha_j \boldsymbol{\eta}_j \otimes \boldsymbol{\eta}_j = \mathbf{M} \right\} \tag{20}$$

$$= \min \left\{ \sum_{j=1}^m \psi(\boldsymbol{\eta}_j) \mid \boldsymbol{\eta}_j \in \mathbb{R}_*^n, \sum_{j=1}^m \boldsymbol{\eta}_j \otimes \boldsymbol{\eta}_j = \mathbf{M} \right\}. \tag{21}$$

Here again $m = (n^2 - n)/2$ by the standard theory of finite-dimensional convexity and the fact that \mathbb{K}_*^n lies in an $(m - 1)$ -dimensional affine subspace of $\mathbb{R}^{n \times n}$. In fact, we may extend ψ to $\psi : \mathbb{R}_*^n \rightarrow \mathbb{R}$ naturally such that $\psi(\alpha \boldsymbol{\eta}) = \alpha^2 \psi(\boldsymbol{\eta})$, and similarly we may extend Ψ into $\Psi : \mathbb{P}_*^n \rightarrow \mathbb{R}$ such that $\Psi(\alpha \mathbf{M}) = \alpha \Psi(\mathbf{M})$ for $\alpha \geq 0$. Formula (21) [cf. also Eq. (3)] is obtained by extending Eq. (20) homogeneously.

Theorem 5.2. *We have the formula $w^{\text{low}}(\mathbf{c}) = \Psi(\mathbf{M}(\mathbf{c}))$.*

The proof follows by combining Proposition 5.1 with the Krein–Milman theorem and by the definition of Ψ .

5.2. The Reuß bound

Above we discussed the lower bound w^{low} to w_{mix} by considering an outer approximation to $\mathcal{H}(\mathbf{c})$. In the examples section we will examine the quality of this bound. Before doing so however, we will briefly consider another lower bound. The upper bound which we have discussed respects the notion of compatibility of the microstructural displacement field through the explicit presence of $\boldsymbol{\varphi} \in \mathcal{W}_{\text{per}}^{1,2}(Q^d)$ in Eq. (7) and the lower bound discussed attempts to be as faithful to compatibility as possible. If however we explicitly remove the compatibility restriction and perform the minimization over the (larger) set of all symmetric gradient fields, then we will obtain a lower bound to the free energy of mixing—a different one from that obtained in the previous section. We call this lower bound the Reuß bound; note $w_{\text{mix}}(\mathbf{c}) \geq w^{\text{low}}(\mathbf{c}) \geq w_{\text{Reuß}}(\mathbf{c})$.

In practical terms we can carry out this minimization by considering the term in Eq. (8) and minimizing over $\boldsymbol{\gamma} = \bar{\boldsymbol{\gamma}}^T \in \mathbb{C}^{d \times d}$ instead of over $i \boldsymbol{\xi} \otimes_{\text{sym}} \boldsymbol{\varphi}_{\boldsymbol{\xi}}$. If we use the

fact that $\boldsymbol{\chi}(\mathbf{y}) \in \mathcal{P}_{\text{pure}}^n$ gives $\int_{Q^n} \boldsymbol{\chi}(\mathbf{y}) \otimes \boldsymbol{\chi}(\mathbf{y}) \, d\mathbf{y} = \sum_{\boldsymbol{\xi} \in \Gamma} \boldsymbol{\chi}_{\boldsymbol{\xi}} \otimes \boldsymbol{\chi}_{-\boldsymbol{\xi}} = \text{diag}(\mathbf{c})$, then we arrive at the result

$$\begin{aligned} w_{\text{ReuB}}(\mathbf{c}) &= -\hat{\mathbf{G}} : \mathbf{M}(\mathbf{c}) \\ &= -\frac{1}{2} \sum_{j=1}^n c_j \boldsymbol{\varepsilon}_j : \mathbb{C} : \boldsymbol{\varepsilon}_j + \frac{1}{2} \sum_{j=1}^n \sum_{k=1}^n c_j c_k \boldsymbol{\varepsilon}_j : \mathbb{C} : \boldsymbol{\varepsilon}_k, \end{aligned}$$

where $\hat{G}_{jk} = \frac{1}{2} \boldsymbol{\varepsilon}_j : \mathbb{C} : \boldsymbol{\varepsilon}_k$. The importance of this bound is that: (1) it is given in explicit form and (2) as we shall see in this section, it is exact in certain (actually common) circumstances.

The exactness of the bound is closely related with the notion of compatible phases, this means that their transformation strains are symmetrically rank-one connected (denoted for short: sr1c). This is expressed as $\boldsymbol{\varepsilon}_j - \boldsymbol{\varepsilon}_i = \mathbf{a} \otimes_{\text{sym}} \mathbf{b}$ for some vectors $\mathbf{a}, \mathbf{b} \in \mathbb{R}^d$. For $d = 3$ we recall (cf. e.g. Bhattacharya, 1993a)

$$\mathbb{R}_{\text{sym}}^{3 \times 3} \ni \mathbf{A} = \mathbf{a} \otimes_{\text{sym}} \mathbf{b} \Leftrightarrow \text{spec}(\mathbf{A}) = \{\lambda_1, 0, \lambda_3\} \quad \text{with } \lambda_1 \leq 0 \leq \lambda_3. \tag{22}$$

The following proposition shows that sr1c transformation strains play a central role as they achieve the lowest possible value for the function ψ .

Proposition 5.3. *If $\boldsymbol{\varepsilon}^\eta = \sum_{j=1}^n \eta_j \boldsymbol{\varepsilon}_j$ satisfies $\boldsymbol{\varepsilon}^\eta = \mathbf{a} \otimes_{\text{sym}} \mathbf{b}$, then*

$$\psi(\boldsymbol{\eta}) = -\boldsymbol{\eta} \cdot \hat{\mathbf{G}} \boldsymbol{\eta} = -\hat{\mathbf{G}} : (\boldsymbol{\eta} \otimes \boldsymbol{\eta}) = -\frac{1}{2} \boldsymbol{\varepsilon}^\eta : \mathbb{C} : \boldsymbol{\varepsilon}^\eta.$$

Proof. Using the ReuB bound we know $\psi(\boldsymbol{\eta}) \geq -\frac{1}{2} \boldsymbol{\varepsilon}^\eta : \mathbb{C} : \boldsymbol{\varepsilon}^\eta$. We define $g(\boldsymbol{\omega}) = -\mathbf{G} : (\boldsymbol{\eta} \otimes \boldsymbol{\eta}) = -\boldsymbol{\eta} \cdot \mathbf{G}(\boldsymbol{\omega}) \boldsymbol{\eta} = -\frac{1}{2} (\boldsymbol{\omega} \cdot \mathbb{C} : \boldsymbol{\varepsilon}^\eta) \cdot \mathbf{T}(\boldsymbol{\omega})^{-1} (\boldsymbol{\omega} \cdot \mathbb{C} : \boldsymbol{\varepsilon}^\eta)$, then clearly $\psi(\boldsymbol{\eta}) = \inf \{g(\boldsymbol{\omega}) \mid \boldsymbol{\omega} \in \mathbb{S}^{d-1}\}$. We now will show that when $\boldsymbol{\omega} = \mathbf{a}/|\mathbf{a}|$ the equality holds and thus the result will be proved.

For the symmetric acoustic tensor $\mathbf{T}(\boldsymbol{\xi})$ we have the identity

$$\mathbf{w} \cdot \mathbf{T}(\boldsymbol{\xi}) \mathbf{v} = [\boldsymbol{\xi} \otimes_{\text{sym}} \mathbf{w}] : \mathbb{C} : [\boldsymbol{\xi} \otimes_{\text{sym}} \mathbf{v}] \quad \text{for all } \boldsymbol{\xi}, \mathbf{v}, \mathbf{w} \in \mathbb{R}^d.$$

For arbitrary $\mathbf{h} \in \mathbb{R}^d$ we choose $\boldsymbol{\xi} = \mathbf{a}$, $\mathbf{v} = \mathbf{b}$ and $\mathbf{w} = \mathbf{T}(\mathbf{a})^{-1} \mathbf{h}$ and find

$$\begin{aligned} \mathbf{b} \cdot \mathbf{h} &= \mathbf{T}(\mathbf{a}) \mathbf{b} \cdot \mathbf{T}(\mathbf{a})^{-1} \mathbf{h} = [\mathbf{a} \otimes_{\text{sym}} (\mathbf{T}(\mathbf{a})^{-1} \mathbf{h})] : \mathbb{C} : [\mathbf{a} \otimes_{\text{sym}} \mathbf{b}] \\ &= [(\mathbf{T}(\mathbf{a})^{-1} \mathbf{h}) \cdot (\mathbf{a} \cdot \mathbb{C} : [\mathbf{a} \otimes_{\text{sym}} \mathbf{b}])] \\ &= \mathbf{h} \cdot (\mathbf{T}(\mathbf{a})^{-1} (\mathbf{a} \cdot \mathbb{C} : [\mathbf{a} \otimes_{\text{sym}} \mathbf{b}])). \end{aligned}$$

As \mathbf{h} was arbitrary we have $\mathbf{T}(\mathbf{a})^{-1} (\mathbf{a} \cdot \mathbb{C} : [\mathbf{a} \otimes_{\text{sym}} \mathbf{b}]) = \mathbf{b}$ and thus we find

$$\begin{aligned} -2g(\mathbf{a}/|\mathbf{a}|) &= (\mathbf{a} \cdot \mathbb{C} : [\mathbf{a} \otimes_{\text{sym}} \mathbf{b}]) \cdot \mathbf{T}(\mathbf{a})^{-1} (\mathbf{a} \cdot \mathbb{C} : [\mathbf{a} \otimes_{\text{sym}} \mathbf{b}]) \\ &= \mathbf{b} \cdot (\mathbf{a} \cdot \mathbb{C} : [\mathbf{a} \otimes_{\text{sym}} \mathbf{b}]) = [\mathbf{a} \otimes_{\text{sym}} \mathbf{b}] : \mathbb{C} : [\mathbf{a} \otimes_{\text{sym}} \mathbf{b}] \\ &= \boldsymbol{\varepsilon}^\eta : \mathbb{C} : \boldsymbol{\varepsilon}^\eta \end{aligned}$$

and the minimum is attained as desired. \square

From this we derive a nice corollary concerning the achievement for the Reuß bound. If we assume that the Reuß bound is achieved at two points $\mathbf{c}^{(1)}$ and $\mathbf{c}^{(2)}$ and if $\boldsymbol{\varepsilon}^{\mathbf{c}^{(1)}}$ and $\boldsymbol{\varepsilon}^{\mathbf{c}^{(2)}}$ are sr1c, then the Reuß bound holds in fact on the whole segment between $\mathbf{c}^{(1)}$ and $\mathbf{c}^{(2)}$.

Corollary 5.4. *Assume we have $\mathbf{c}^{(j)} \in \mathcal{P}^n$ with $w_{\text{mix}}(\mathbf{c}^{(j)}) = -\hat{\mathbf{G}} : \mathbf{M}(\mathbf{c}^{(j)})$ for $j = 1, 2$. Moreover, assume $\boldsymbol{\varepsilon}^{\mathbf{c}^{(2)} - \mathbf{c}^{(1)}} = \boldsymbol{\varepsilon}^{\mathbf{c}^{(2)}} - \boldsymbol{\varepsilon}^{\mathbf{c}^{(1)}} = \mathbf{a} \otimes_{\text{sym}} \mathbf{b}$. For $\theta \in [0, 1]$ let $\mathbf{c}_\theta = \theta \mathbf{c}^{(1)} + (1 - \theta) \mathbf{c}^{(2)}$, then*

$$w_{\text{mix}}(\mathbf{c}_\theta) = w_{\text{Reuß}}(\mathbf{c}_\theta) = -\hat{\mathbf{G}} : \mathbf{M}(\mathbf{c}_\theta) \quad \text{for } \theta \in [0, 1].$$

Proof. We apply Eq. (15) and Proposition 5.3 to obtain

$$\begin{aligned} w_{\text{mix}}(\mathbf{c}_\theta) &\leq \theta w_{\text{mix}}(\mathbf{c}^{(1)}) + (1 - \theta) w_{\text{mix}}(\mathbf{c}^{(2)}) + \theta(1 - \theta) \psi(\mathbf{c}^{(2)} - \mathbf{c}^{(1)}) \\ &= -\hat{\mathbf{G}} : [\theta \mathbf{M}(\mathbf{c}^{(1)}) + (1 - \theta) \mathbf{M}(\mathbf{c}^{(2)}) \\ &\quad + \theta(1 - \theta)(\mathbf{c}^{(2)} - \mathbf{c}^{(1)}) \otimes (\mathbf{c}^{(2)} - \mathbf{c}^{(1)})]. \end{aligned}$$

With Eq. (14) we conclude $w_{\text{mix}}(\mathbf{c}_\theta) \leq -\hat{\mathbf{G}} : \mathbf{M}(\mathbf{c}_\theta)$. However, the opposite estimate always holds since this is also the Reuß bound. \square

As a second corollary we obtain a result which seems to be well known in the community, but it is not stated like this.

Corollary 5.5. *Assume that all transformation strains $\boldsymbol{\varepsilon}_i$ are pairwise sr1c. Then, the mixture function satisfies $w_{\text{mix}}(\mathbf{c}) = w_{\text{Reuß}}(\mathbf{c}) = -\hat{\mathbf{G}} : \mathbf{M}(\mathbf{c})$ for all $\mathbf{c} \in \mathcal{P}^n$.*

6. Examples

In this section we present three examples demonstrating the use of the analysis developed to this point. In the first example we consider an analytical application of our developments to a particular case that has appeared in the literature for 3-variants and extend it to the case of n -variants. In the second example, we examine the quality of the bounds for a particular material that undergoes a cubic to tetragonal phase transformation; thus this is a problem with 4-variants. Lastly, we demonstrate for illustrative purposes the application of the Reuß bound in an equilibrium evolutionary model.

6.1. Co-linear transformation strains

Proposition 6.1. *If $\psi(\boldsymbol{\eta}) = \mathbf{B} : (\boldsymbol{\eta} \otimes \boldsymbol{\eta})$ for all $\boldsymbol{\eta} \in \mathbb{R}_*^n$ and constant $\mathbf{B} \in \mathbb{R}^{n \times n}$, then $w_{\text{mix}}(\mathbf{c}) = \mathbf{B} : \mathbf{M}(\mathbf{c})$.*

Proof. We first note that in Eq. (21) \mathbf{B} may be factored out of the objective. Using the constraint $\sum \boldsymbol{\eta}_j \otimes \boldsymbol{\eta}_j = \mathbf{M}$ gives $w^{\text{low}}(\mathbf{c}) = \mathbf{B} : \mathbf{M}(\mathbf{c})$.

To complete the proof we now show that w^{low} is also an upper bound. Since $w^{\text{low}}(\mathbf{e}_j) = 0$ it remains to verify Eq. (19). However, using Eq. (14) and the special form of w^{low} we immediately obtain Eq. (19) (with equality). \square

In fact, the assumption can be weakened severely by assuming $\psi(\boldsymbol{\eta}) \geq \mathbf{B} : (\boldsymbol{\eta} \otimes \boldsymbol{\eta})$ with equality only for those $\boldsymbol{\eta}$ used in the construction in Eq. (18).

The n -well problem can now be solved explicitly, when all transformation strains lie on one straight line in $\mathbb{R}_{\text{sym}}^{d \times d}$, i.e., $\boldsymbol{\varepsilon}_j = \boldsymbol{\varepsilon}_0 + a_j \hat{\boldsymbol{\varepsilon}}$ with $a_j \in \mathbb{R}$, and $\boldsymbol{\varepsilon}_0, \hat{\boldsymbol{\varepsilon}} \in \mathbb{R}_{\text{sym}}^{d \times d}$ given constants. The case $\boldsymbol{\varepsilon}_1 = -\boldsymbol{\varepsilon}_3$ and $\boldsymbol{\varepsilon}_2 = \mathbf{0}$ is considered in Pagano et al. (1998). For $\boldsymbol{\varepsilon}^n = \sum_j \eta_j \boldsymbol{\varepsilon}_j$ with $\boldsymbol{\eta} \otimes \boldsymbol{\eta} \in \mathbb{E}_*^n$ we find $\boldsymbol{\varepsilon}^n = (\boldsymbol{\eta} \cdot \mathbf{a}) \hat{\boldsymbol{\varepsilon}}$ and

$$\psi(\boldsymbol{\eta}) = -\frac{\gamma}{2} (\mathbf{a} \cdot \boldsymbol{\eta})^2 = -\frac{\gamma}{2} (\mathbf{a} \otimes \mathbf{a}) : (\boldsymbol{\eta} \otimes \boldsymbol{\eta}),$$

$$\text{where } \gamma = \max\{(\boldsymbol{\omega} \cdot \mathbb{C} : \hat{\boldsymbol{\varepsilon}}) \cdot \mathbf{T}(\boldsymbol{\omega})^{-1}(\boldsymbol{\omega} \cdot \mathbb{C} : \hat{\boldsymbol{\varepsilon}}) \mid \boldsymbol{\omega} \in \mathbb{S}^{d-1}\}.$$

With Proposition 6.1 we conclude the following exact formula.

Theorem 6.2. *If all $W(\boldsymbol{\varepsilon}, \mathbf{e}_j)$ have form (6) with $\boldsymbol{\varepsilon}_j = \boldsymbol{\varepsilon}_0 + a_j \hat{\boldsymbol{\varepsilon}}$, then*

$$w_{\text{mix}}(\mathbf{c}) = -\frac{\gamma}{2} (\mathbf{a} \otimes \mathbf{a}) : \mathbf{M}(\mathbf{c}) = -\frac{\gamma}{2} \left[\sum_{j=1}^n a_j^2 c_j - (\mathbf{a} \cdot \mathbf{c})^2 \right].$$

This result is also a generalization of Proposition 8.1 in Kohn (1991) which treats the case of hydrostatic transformation strains (i.e. $\boldsymbol{\varepsilon}_0 = \mathbf{0}$ and $\hat{\boldsymbol{\varepsilon}} = \mathbf{1}$).

6.2. Cubic to tetragonal phase transformation (isotropic case)

We now consider a special case which relates to the cubic to tetragonal phase transformation in shape memory alloys. There are four phases, three variants of martensite ($i = 1, 2, 3$) and one austenite ($i = 4$) with transformation strains

$$\boldsymbol{\varepsilon}_1 = \text{diag}(\beta, \alpha, \alpha), \quad \boldsymbol{\varepsilon}_2 = \text{diag}(\alpha, \beta, \alpha), \quad \boldsymbol{\varepsilon}_3 = \text{diag}(\alpha, \alpha, \beta), \quad \boldsymbol{\varepsilon}_4 = \mathbf{0}.$$

Here the constants $\alpha, \beta \in \mathbb{R}$ usually are such that $2\alpha + \beta$ is much smaller than $|\alpha| + |\beta|$. For instance, for some shape memory alloys we have $(\alpha, \beta) = (-0.0608, 0.1302)$ for Ni–36.8Al, $(0.0868, -0.1497)$ for Fe–25Pt, and $(0.1241, -0.1941)$ for Fe–30Ni–0.3C (see e.g. Bhattacharya and Kohn, 1996).

By Eq. (22) we easily see that the martensite phases as defined above are sr1c with each other for these materials. Moreover, certain combinations of martensites may be sr1c to the austenite phase. This is the case if and only if

$$\alpha\beta < 0 \quad \text{and} \quad 0 < |\alpha| < |\beta|.$$

These conditions seem to be satisfied for all cubic to tetragonal phase transformations. They guarantee that $\theta_k \boldsymbol{\varepsilon}_i + (1 - \theta_k) \boldsymbol{\varepsilon}_j$ is sr1c to $\boldsymbol{\varepsilon}_4$ for $\theta_k \in \{\alpha/(\alpha - \beta), \beta/(\beta - \alpha)\}$ and $i \neq j \in \{1, 2, 3\}$. Note that the polytope $\mathcal{P} \subset \mathbb{R}^4$ in this situation can be viewed as a subset of \mathbb{R}^3 embedded in \mathbb{R}^4 ; see the upper-left sector of Fig. 1. If we consider it

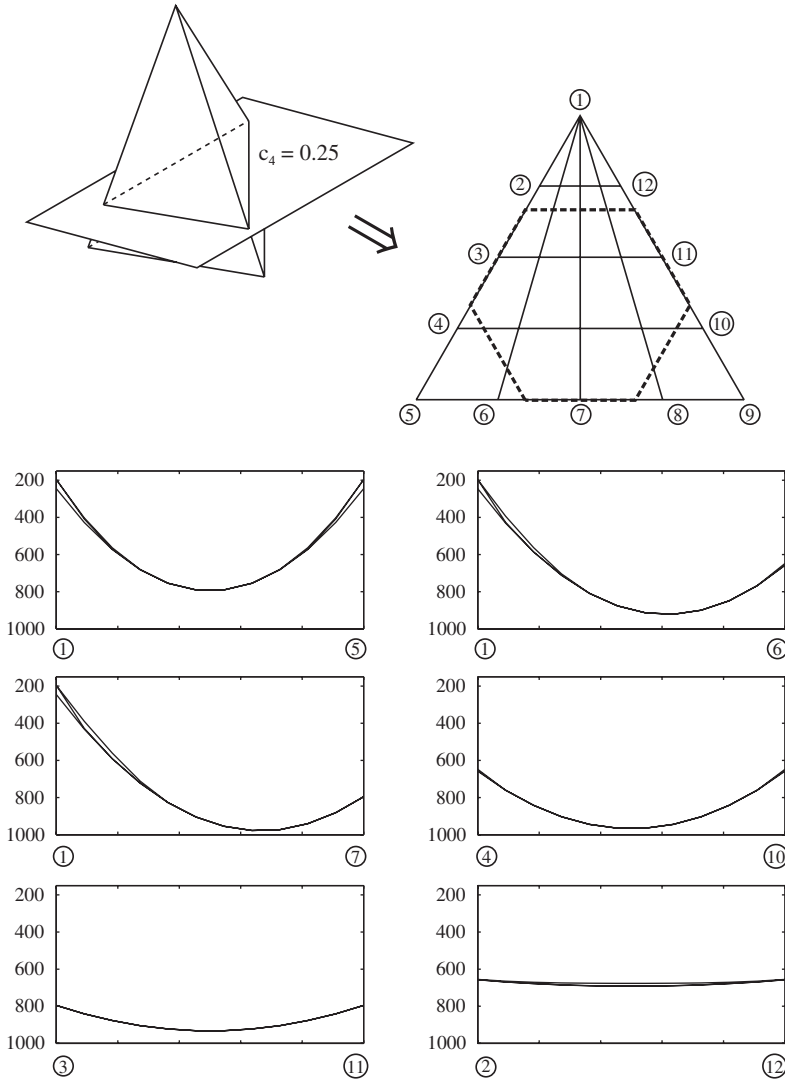


Fig. 1. Comparison of mixing energy bounds for a fixed austenite phase fraction $c_4 = 0.25$. The top curve is the lamination bound, the middle curve is the \mathbb{H} -measure lower bound, and the lower curve is the Reuß lower bound.

as an object in \mathbb{R}^3 , then the six points $\theta_k \mathbf{e}_i + (1 - \theta_k) \mathbf{e}_j$ define a hexagon \mathbf{H} on the face of the polytope \mathcal{P} which is spanned by the three corners \mathbf{e}_1 , \mathbf{e}_2 , and \mathbf{e}_3 . Taking into account the additional point \mathbf{e}_4 we can then define a hexagonal pyramid inside the polytope \mathcal{P} . Applying Corollary 5.4 we find

Proposition 6.3. *Inside the hexagonal pyramid we have $w_{\text{mix}} = w_{\text{Reuß}}$.*

Although the above result holds for general (but identical) elasticity tensor \mathbb{C} , we assume that the elasticity tensor is isotropic: $\mathbb{C} : \boldsymbol{\varepsilon} = \lambda \operatorname{tr}(\boldsymbol{\varepsilon}) \mathbf{1} + 2\mu \boldsymbol{\varepsilon}$. This assumption makes our example slightly academic but nevertheless we are able to obtain interesting features and are able to give explicit formulae. The acoustic tensor reads

$$\mathbf{T}(\boldsymbol{\omega}) = \mu \mathbf{1} + (\lambda + \mu) \boldsymbol{\omega} \otimes \boldsymbol{\omega}, \quad \mathbf{T}(\boldsymbol{\omega})^{-1} = \frac{1}{\mu} \mathbf{1} - \frac{\lambda + \mu}{\mu(\lambda + 2\mu)} \boldsymbol{\omega} \otimes \boldsymbol{\omega}.$$

For convenience, we define $a = -1/2\mu$ and $b = (\lambda + \mu)/2\mu(\lambda + 2\mu)$ and note that $a + b = -1/(2\lambda + 4\mu) < 0$.

The function ψ can now be evaluated as follows:

Proposition 6.4. *Let $\sigma_j \in \mathbb{R}, j=1,2,3$, be the eigenvalues of the symmetric tensor $\mathbb{C} : \boldsymbol{\varepsilon}^n$ and σ_{\min} and σ_{\max} the smallest and largest eigenvalues. Then, $\psi(\boldsymbol{\eta}) = \gamma(\sigma_{\min}, \sigma_{\max})$ with $\gamma(s, t) = (a + b) \max\{s^2, t^2\}$ for $b \leq 0$ and*

$$\begin{aligned} \gamma(s, t) &= \frac{a + b}{2} (s^2 + t^2) - \frac{(a + b)^2}{4b} (s + t)^2 - \frac{b}{4} (s - t)^2 \\ &\quad + \frac{1}{4b} (\max\{0, |a + b| |s + t| - b|s - t|\})^2 \quad \text{for } b > 0. \end{aligned}$$

Proof. We have $\psi(\boldsymbol{\eta}) = \min\{\hat{t}(\boldsymbol{\omega}, \boldsymbol{\eta}) : \boldsymbol{\omega} \in \mathbb{S}^2\}$ with $\hat{t}(\boldsymbol{\omega}, \boldsymbol{\eta}) = -\frac{1}{2}(\boldsymbol{\omega} \cdot \mathbb{C} : \boldsymbol{\varepsilon}^n) \cdot \mathbf{T}(\boldsymbol{\omega})^{-1}(\boldsymbol{\omega} \cdot \mathbb{C} : \boldsymbol{\varepsilon}^n)$. By isotropy it is sufficient to consider only the case $\mathbb{C} : \boldsymbol{\varepsilon}^n = \operatorname{diag}(\boldsymbol{\sigma}) = \operatorname{diag}(\sigma_1, \sigma_2, \sigma_3)$. Then,

$$\hat{t}(\boldsymbol{\omega}, \boldsymbol{\eta}) = a |\operatorname{diag}(\boldsymbol{\sigma}) \boldsymbol{\omega}|^2 + b (\boldsymbol{\omega} \cdot \operatorname{diag}(\boldsymbol{\sigma}) \boldsymbol{\omega})^2 = a \sum_{i=1}^3 \sigma_i^2 \omega_i^2 + b \left[\sum_{i=1}^3 \sigma_i \omega_i^2 \right]^2.$$

With $\Delta = \{\mathbf{y} \in \mathbb{R}^3 \mid y_i \geq 0, y_1 + y_2 + y_3 = 1\}$ we now define

$$g(\boldsymbol{\sigma}, \mathbf{y}) = a \sum_{i=1}^3 \sigma_i^2 y_i + b \left[\sum_{i=1}^3 \sigma_i y_i \right]^2 \quad \text{and} \quad \Gamma(\boldsymbol{\sigma}) = \min\{g(\boldsymbol{\sigma}, \mathbf{y}) \mid \mathbf{y} \in \Delta\}$$

such that it remains to show $\gamma(\sigma_{\min}, \sigma_{\max}) = \Gamma(\boldsymbol{\sigma})$. The case $b \leq 0$ is treated easily as $g(\boldsymbol{\sigma}, \cdot) : \Delta \rightarrow \mathbb{R}$ is concave and, hence, assumes its minimum in one of the extremal points by the Krein–Milman theorem. Clearly $\Gamma(\boldsymbol{\sigma}) = \min\{g(\boldsymbol{\sigma}, \mathbf{e}_j) \mid j = 1, 2, 3\}$ is the desired result (recall $a + b < 0$).

In the case $b > 0$ the function $g(\boldsymbol{\sigma}, \cdot)$ is convex, however it is easy to see (as $D_{\mathbf{y}}^2 g$ has rank one) that the minimum is also attained on the boundary of Δ . This leads to a minimization on three intervals, each leading to the result $\gamma(\sigma_i, \sigma_j)$ with γ as defined above. We use $\min\{s\theta + t\theta^2 \mid \theta \in [0, 1]\} = \frac{1}{2}[s + t + t w((t + s)/t)]$ with $w(\tau) = \frac{1}{2}[\tau^2 + 1 - \max\{0, |\tau| - 1\}^2]$, and apply it to the restriction of $g(\boldsymbol{\sigma}, \cdot)$ to each of the boundary segments.

It remains to show that the minimum is achieved on the side connecting the largest and the smallest eigenvalues. To this end note that $\gamma(\cdot, t)$ is increasing on $(-\infty, t]$ and

decreasing on $[t, \infty)$. This implies, for $\sigma_i \leq \sigma_j$, the inequality

$$\gamma(\sigma_i, \sigma_j) \geq \max\{\gamma(\sigma_{\min}, \sigma_j), \gamma(\sigma_i, \sigma_{\max})\}.$$

This establishes the result. \square

In our special situation the eigenvalues σ_j of $\mathbb{C} : \boldsymbol{\varepsilon}^\eta$ are easily obtained, since $\mathbb{C} : \boldsymbol{\varepsilon}^\eta$ is always diagonal: $\text{diag}(\boldsymbol{\sigma})$. Employing the matrix

$$\mathbf{B} = \lambda(\beta + 2\alpha) \begin{pmatrix} 1 & 1 & 1 & 0 \\ 1 & 1 & 1 & 0 \\ 1 & 1 & 1 & 0 \end{pmatrix} + 2\mu \begin{pmatrix} \beta & \alpha & \alpha & 0 \\ \alpha & \beta & \alpha & 0 \\ \alpha & \alpha & \beta & 0 \end{pmatrix}$$

we find $\boldsymbol{\sigma} = \mathbf{B}\boldsymbol{\eta}$. Together with $\bar{\sigma} = [\lambda(\beta + 2\alpha) + 2\mu\alpha](\eta_1 + \eta_2 + \eta_3)$ we obtain the formula

$$\psi(\boldsymbol{\eta}) = \gamma(\sigma_{\min}, \sigma_{\max})$$

with

$$\sigma_{\min} = \bar{\sigma} + 2\mu \min\{(\beta - \alpha)\eta_j \mid j = 1, 2, 3\},$$

$$\sigma_{\max} = \bar{\sigma} + 2\mu \max\{(\beta - \alpha)\eta_j \mid j = 1, 2, 3\}.$$

This provides an explicit formula for the evaluation of the function ψ . Interestingly enough we see that ψ is defined piecewise by quadratic functions.

To assess the quality of the expressions for the bounds we have utilized this expression for $\psi(\boldsymbol{\eta})$ to compute the \mathbb{H} -measure lower bound derived in Section 5.1. In the computation, we utilize Eq. (21) which amounts to a 24-dimensional optimization problem subject to 6 linear and 12 quadratic constraints. The algorithm employed is a sequential quadratic programming algorithm. These computations are then compared to the lamination upper bound (using 2-lamination steps) and to the Reuß lower bound. These results are shown in Figs. 1–3 for an Ni–36.8Al alloy assuming $\lambda = 97.8 \text{ kN/mm}^2$ and $\mu = 53.6 \text{ kN/mm}^2$. Each figure represents a fixed value of the austenite phase fraction. In the upper left-hand corner of each figure, one finds a representation of the polytope \mathcal{P} with the top point representing austenite \mathbf{e}_4 and a cutting plane at a fixed value of phase fraction as indicated. In the upper right-hand corner of each figure, one finds a plot of the intersection of the cutting plane with the polytope. On the intersection, we have also plotted the intersection of the cutting plane with the hexagonal pyramid as a dotted line. The 12 labelled points are used to define rays on the cutting plane over which we plot the mixing energy. Six such plots are shown in the lower half of each figure. The top curve in each plot corresponds to the lamination upper bound, the middle curve corresponds to the \mathbb{H} -measure bound, and the lower curve corresponds to the Reuß bound. As can be seen from the figures, the Reuß bound is indeed exact inside the hexagonal pyramid; in fact all three bounds are exact there. Outside of the hexagonal pyramid, we can see that there is some deterioration of the Reuß bound but it is still quite reasonable. The \mathbb{H} -measure lower bound is very close



Fig. 2. Comparison of mixing energy bounds for a fixed austenite phase fraction $c_4 = 0.50$. The top curve is the lamination bound, the middle curve is the \mathbb{H} -measure lower bound, and the lower curve is the Reuß lower bound.

to the lamination upper bound inside the pyramid (where it is exact) and also outside the pyramid—indicating that these two bounds are quite sharp for the case examined.

6.3. Evolutionary example utilizing the Reuß bound

Lastly, to demonstrate a practical application of mixture energy bounds, the Reuß estimate is employed in the numerical realization of a fully relaxed shape memory

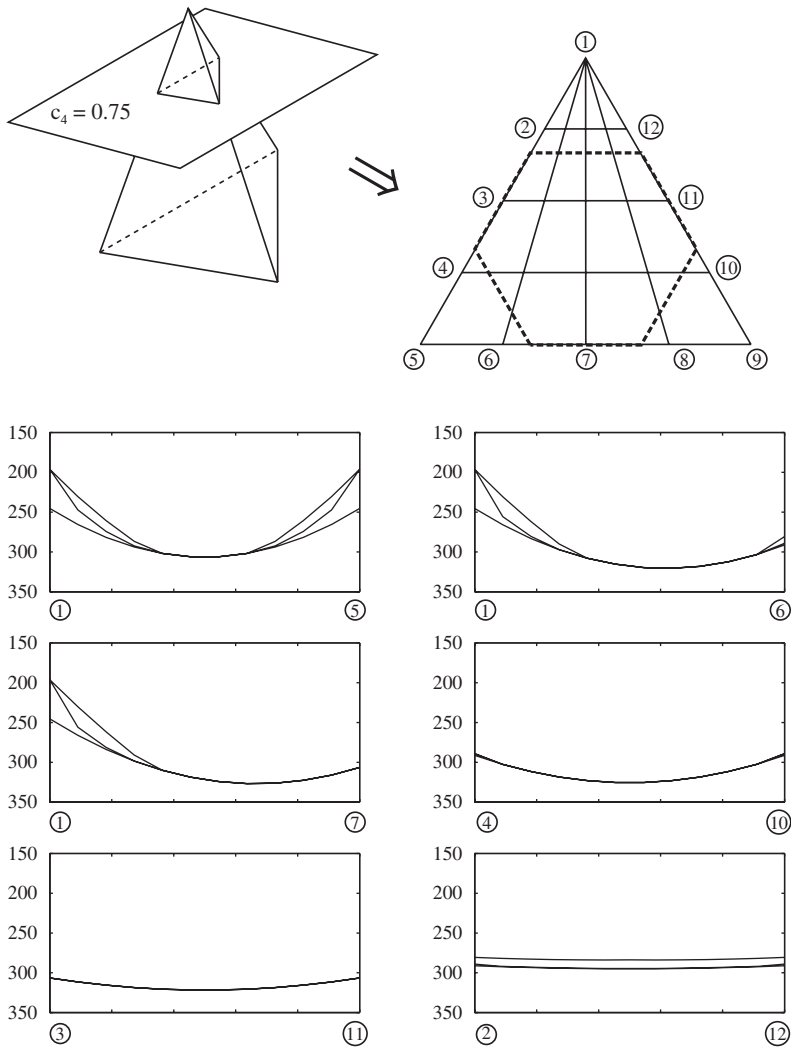


Fig. 3. Comparison of mixing energy bounds for a fixed austenite phase fraction $c_4 = 0.75$. The top curve is the lamination bound, the middle curve is the \mathbb{H} -measure lower bound, and the lower curve is the Reuß lower bound.

alloy model. The predictions based on this model correspond well with the results obtained from experimental tests of single crystal specimens. The model is briefly described below. For a more complete discussion see Hall and Govindjee (2002); see, also, Govindjee and Miehe (2001) for a discussion of a similar model but with hysteresis.

Table 1
Constitutive equations

(1) Free energy functions:	$QW(\boldsymbol{\varepsilon}, \mathbf{c}) = \sum_{i=1}^n c_i W(\boldsymbol{\varepsilon}, \mathbf{e}_i) + w_{\text{Reuß}}(\mathbf{c})$	(23)
(2) Volume fractions:	$\mathbf{c}^*(\boldsymbol{\varepsilon}) = \arg \min \{ QW(\boldsymbol{\varepsilon}, \mathbf{c}) \mid \mathbf{c} \in \mathcal{P}^n \}$	(24)
(3) Stress:	$\mathbf{s} = \sum_{i=1}^n c_i^* \mathbf{s}_i \quad \text{with } \mathbf{s}_i = \mathbb{C} : (\boldsymbol{\varepsilon} - \boldsymbol{\varepsilon}_i)$	(25)

6.3.1. Relaxed single crystal model

With given bounds on the mixture energy, it is possible to construct a model strictly from the viewpoint of elastic stability. In this section the equations for one such model are briefly presented. The model is summarized in Table 1, where the partially relaxed free energy is given in Eq. (23) and employs the Reuß term for the mixing energy.

In Hall and Govindjee (2002), the thermal terms are given explicitly to allow for the simulation of thermomechanical problems. Here, we simplify the presentation and note that all examples will be conducted at a fixed temperature above the austenite finish temperature where $\alpha_n < \alpha_i$ for $i \in \{1, \dots, n-1\}$; n is understood to correspond to the austenite variant and $\alpha_j = \alpha_i$ for $i, j \in \{1, \dots, n-1\}$. This partially relaxed free energy allows for the determination of the volume fractions as a function of the strain path through the optimization problem of Eq. (24). Finally, the stress is specified in Eq. (25) as a function of the strain and phase fractions. Note that at a fixed temperature, the only parameters in the model are the elastic moduli and the transformation strains. Details of the conditions under which a solution to the relaxation step exists, treatment of the numerical implementation issues, and the overall behavior of the model are more fully discussed in Hall and Govindjee (2002).

6.3.2. Single crystal simulation

One of the most striking aspects of experimental data on shape memory single crystals is the strong dependence of the phase transformation properties on the crystallographic orientation of the test specimen. It is shown below that this physically observed behavior is captured by the mixture energy bounds as incorporated into the model of Table 1. This is demonstrated by simulating the response of uniaxial tensile specimens over a representative set of directions with respect to the parent lattice. The material under consideration is a Cu–Al–Ni alloy undergoing a $\beta_1 \rightarrow \gamma'_1$ stress-induced phase change.¹ In this case, the symmetry change is from a cubic (DO₃) parent phase to six variants of an orthorhombic martensite where each of the martensite variants is twin compatible with one another in the rank-one sense, see Eq. (22). The estimated material parameters for this material are those specified in Hall and Govindjee (2002).

The simulation procedure is as follows. First, specimen dimensions were chosen to be of comparable dimensions to those typically used in the experimental literature.

¹ The twinning characteristics of this particular material have been studied in detail in the work of Ichinose et al. (1985) and Okamoto et al. (1986).

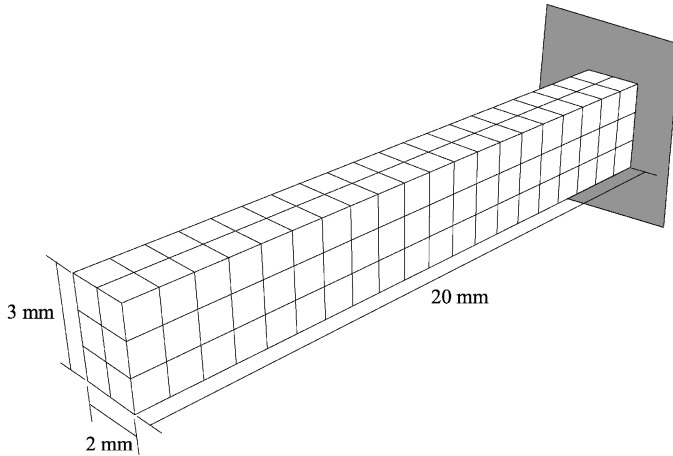


Fig. 4. Dimensions and mesh of the simulated specimen.

Fig. 4 shows the dimensions and the finite element mesh used for all of the examples (again, see Hall and Govindjee (2002) for details). To reproduce the most common experimental boundary conditions, one end of the mesh was fixed while the other underwent an imposed displacement along the major axis of the specimen. The examination of orientation dependence followed by creating a discretization of approximately 80 points in the $[(0, 0, 1)\beta_1; (0, 1, 0)\beta_1; (\bar{1}, 1, 1)\beta_1]$ -region of a standard stereographic projection.² For each point on the stereographic projection, a properly oriented tensile specimen was generated and simulated under tension using a finite element approximation. The tests were all pseudoelastic at constant temperature above the “austenite finish”.

To give an idea of the variation of the overall mechanical response with respect to orientation, Fig. 5 shows the calculated behavior of specimens whose tensile axes coincide with the indicated points in the stereographic plane of the parent lattice. In this plot, the infinitesimal strain and stress data were computed from the end response of the bars in each simulation; this is of importance because of the strong effect of the end conditions on the response of the specimen. Note that both the “transformation stress” (estimated using the offset method) and the “apparent recoverable strain” (estimated by the region bounded by elastic behaviors) vary with respect to orientation. The qualifier “apparent” is used here to distinguish the experimental and simulated response from the recoverable strain predictions made by the crystallographic theory.

An interesting aspect of the computed response is the inverse relation between the length of the apparent yield plateau and the transformation stress level. This can be seen by comparing Figs. 6 and 7 which show the variation of transformation strain with orientation and the variation of transformation stress with orientation, respectively.

² Here, the $(\cdot, \cdot, \cdot)\beta_1$ notation indicates integers locating a *direction* in the crystal with respect to the β_1 phase basis vectors; see e.g. Kelley and Groves (1970), Sands (1975) and Khachaturyna (1983).

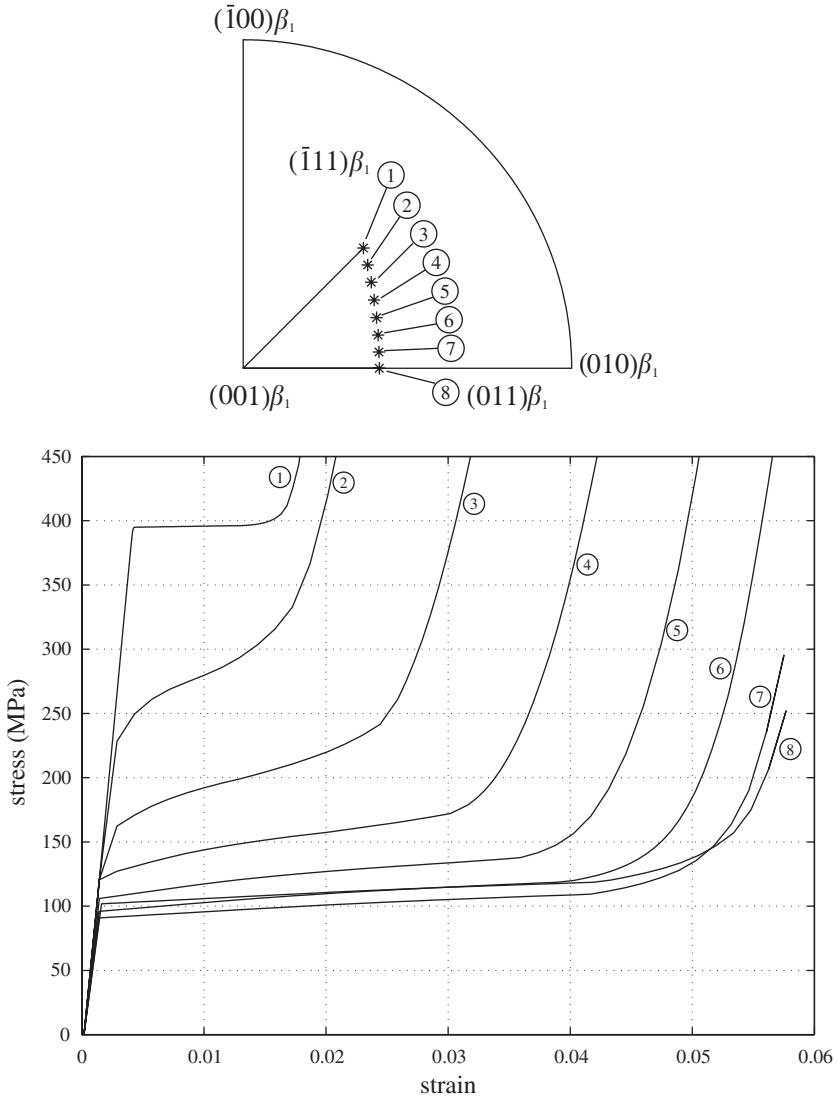


Fig. 5. Variation of mechanical response along the indicated directions in the stereographic plane.

For example, the $(\bar{1}, 1, 1)\beta_1$ direction was computed to have the highest transformation stress in the region and a low transformation strain. Similarly, the greatest apparent recoverable strain computed was located in the $(0, 1, 1)\beta_1$ direction which had a low transformation stress.

In Table 2 the simulations are compared with well-established data regarding the recoverable strain. The first data row is reproduced from Table IV of Nenno and Saburi

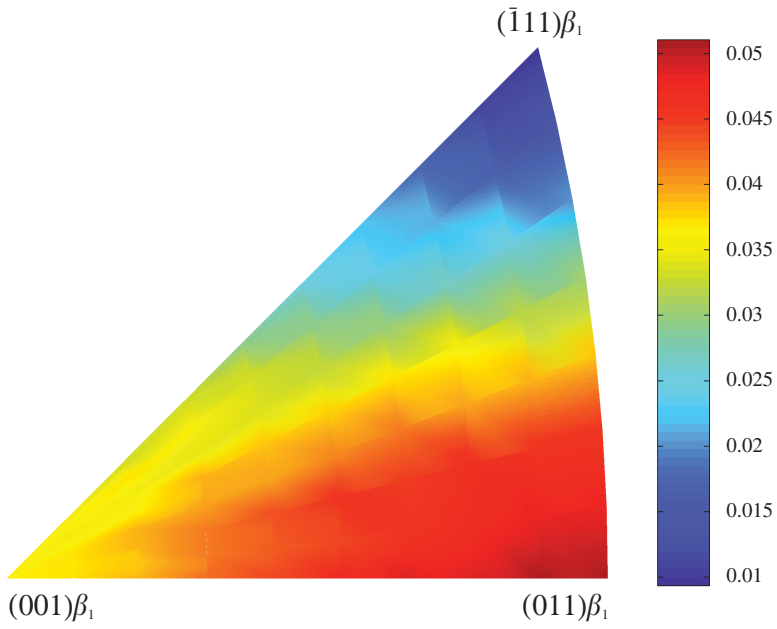


Fig. 6. Apparent transformation strain as a function of orientation.

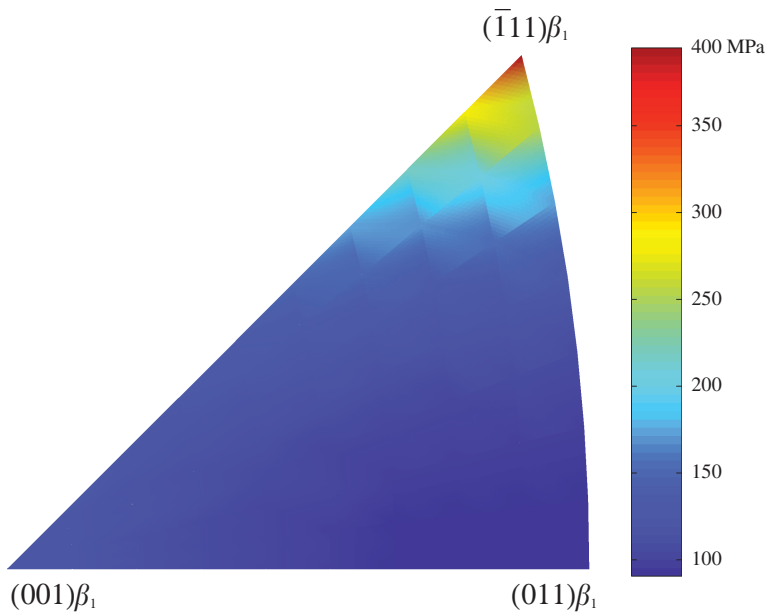


Fig. 7. Transformation stress as a function of specimen orientation.

Table 2
Recoverable strain

Direction	$(0, 0, 1)\beta_1$ (%)	$(0, 1, 1)\beta_1$ (%)	$(\bar{1}, 1, 1)\beta_1$ (%)
Bound	4.3	6.2	1.6
Simulation	3.6	5.1	1.0

Table 3
Transformation stress (MPa), 0.1% offset

Direction	$(0.925, 0.380, 0.000)\beta_1$	$(-0.447, -0.447, 0.775)\beta_1$	$(-0.577, -0.577, 0.577)\beta_1$
Experiment	105	170	400
Simulation	100	180	395

(1981), wherein the maximum recoverable strain of single crystal (orthorhombic) Cu–Al–Ni is listed for the indicated directions based on the established lattice parameters of each phase. Although based on experimentally determined single crystal data, their recoverable strain values rely on a thought experiment involving idealized homogeneous tensile conditions and a solely kinematic, albeit finite deformation, computation. Hence, Nenno and Saburi (1981) should serve as an upper bound for our simulations. While this is in fact the case, it is more noteworthy that the simulations follow the trends established by their upper bound with regard to direction and the relative magnitudes of the recoverable strain.

A similar comparison is made for transformation stress levels in Table 3 wherein the transformation stress levels are compared for three directions for which experimental data are available. The transformation stress was estimated from the response curves for both the experimental and simulated data by using a 0.1% strain offset to estimate the start of the phase transformation. The close match for initiation of the phase change is an indicator that the Reuß mixture energy bound has captured the essential features of the transformation energetics.³

Acknowledgements

SG dankt der Alexander von Humboldt–Stiftung für die Verleihung eines Forschungsstipendium an der Universität Stuttgart. SG also acknowledges the support of the Lawrence Livermore National Laboratory through subcontract B502681 of DOE prime contract W-7405-ENG-48. The research of AM was partially supported by DFG through project C7 of SFB 404 (Multifield Problems).

³ Detailed comparisons with the experimental work of Shield (1995) are made in Hall and Govindjee (2002).

References

- Avellaneda, M., Milton, G., 1989. Bounds on the effective elasticity tensor of composites based on two-point correlations. In: Hui, D., Koszic, T. (Eds.), *Proceedings of the ASME Energy-Technology Conference and Exposition*. ASME, New York.
- Ball, J., James, R., 1987. Fine phase mixtures as minimizers of energy. *Arch. Rational Mech. Anal.* 100, 13–52.
- Ball, J., James, R., 1992. Proposed experimental tests of a theory of fine microstructures and the 2-well problem. *Philos. Trans. R. Soc. London A* 338, 389–450.
- Bhattacharya, K., 1993a. Comparison of the geometrically nonlinear and linear theories of martensitic transformations. *Contin. Mech. Thermodyn.* 5, 205–242.
- Bhattacharya, K., 1993b. The microstructure of martensite and its implications for the shape-memory effect. In: Kinderlehrer, D., James, R., Luskin, M., Eriksen, J. (Eds.), *Microstructure and Phase Transition*. Springer, New York, pp. 1–25.
- Bhattacharya, K., James, R., 1999. A theory of thin films of martensitic materials with applications to microactuators. *J. Mech. Phys. Solids* 47, 531–576.
- Bhattacharya, K., Kohn, R., 1995. Recoverable strains in shape-memory alloys. *J. Phys. IV* 5, C8–261–C8–266.
- Bhattacharya, K., Kohn, R., 1996. Symmetry, texture and the recoverable strain of shape-memory polycrystals. *Acta Mater.* 44, 529–542.
- Bhattacharya, K., James, R., Swart, P., 1997. Relaxation in shape-memory alloys. Part I: basic model. *Acta Mater.* 45, 4547–4560.
- Boyd, J., Lagoudas, D., 1996. A thermodynamic constitutive model for the shape memory materials. Part I: the monolithic shape memory alloy. *Int. J. Plasticity* 12, 805–842.
- Carstensen, C., Plecháč, P., 2001. Numerical analysis of a relaxed variational model of hysteresis in two-phase solids. *Math. Model. Numer. Anal.* 35, 865–878.
- Dacorogna, B., 1989. *Direct Methods in the Calculus of Variations*. Springer, Berlin.
- Firoozye, N., 1991. Optimal use of the translation method and relaxations of variational problems. *Comm. Pure Appl. Math.* 44, 643–678.
- Goldsztein, G., 2001. The effective energy and laminated microstructures in martensitic phase transformations. *J. Mech. Phys. Solids* 49, 899–925.
- Govindjee, S., Miehe, C., 2001. A multi-variant martensitic phase transformation model: formulation and numerical implementation. *Comput. Methods Appl. Mech. Eng.* 191, 215–238.
- Hall, G., Govindjee, S., 1999. A model and numerical framework for the simulation of solid-solid phase transformations. Technical Report UCB/SEMM-1999/11, Department of Civil Engineering, University of California, Berkeley.
- Hall, G., Govindjee, S., 2002. Application of a partially relaxed shape memory free energy function to estimate the phase diagram and predict global microstructure evolution. *J. Mech. Phys. Solids* 50, 501–530.
- Huang, M., Brinson, L., 1998. A multivariant model for single crystal shape memory alloy behavior. *J. Mech. Phys. Solids* 46, 1379–1409.
- Ichinose, S., Funatsu, Y., Otsuka, K., 1985. Type II deformation twinning in γ'_1 martensite in a Cu–Al–Ni alloy. *Acta Metal.* 33, 1613–1620.
- Kelley, A., Groves, G., 1970. *Crystallography and Crystal Defects*. TechBooks, Herndon, VA.
- Khachaturyana, A., 1983. *Theory of Structural Transformations in Solids*. Wiley, New York.
- Kohn, R., 1991. The relaxation of a double-well problem. *Contin. Mech. Thermodyn.* 3, 193–236.
- Kuczma, M., Mielke, A., Stein, E., 1999. Modelling of hysteresis in two-phase systems. *Arch. Mech.* 51, 693–715.
- Levitas, V., 1998. Thermomechanical theory of martensitic phase transformations in inelastic materials. *Int. J. Solids Structures* 35, 889–940.
- Mielke, A., 2000. Estimates on the mixture function for multiphase problems in elasticity. In: *Multifield Problems*. Springer, Berlin, pp. 96–103, Carnegie–Mellon University, Pittsburgh, PA.

- Mielke, A., 2002. Evolution of rate-independent inelasticity with microstructure using relaxation and Young measures. In: Miehe, C. (Ed.), Proceedings of the IUTAM Symposium Computational Mechanics of Solid Materials at Large Strains, Stuttgart, August 2001. Kluwer, Dordrecht, in press.
- Mielke, A., Theil, F., 1999. A mathematical model for rate-independent phase transformations with hysteresis. In: Alber, H.-D., Balean, R., Farwig, R. (Eds.), Models of Continuum Mechanics in Analysis and Engineering. Shaker, Berlin, pp. 117–129.
- Mielke, A., Theil, F., Levitas, V., 1998. Mathematical formulation of quasistatic phase transformations with friction using an extremum principle. Technical Report Preprint IfAM, Universität Hannover.
- Mielke, A., Theil, F., Levitas, V., 2002. A variational formulation of rate-independent phase transformations with friction using an extremum principle. Arch. Rational Mech. Anal. 162, 137–177.
- Müller, I., Xu, H., 1991. On the pseudo-elastic hysteresis. Acta Metal. 39, 263–271.
- Nenno, S., Saburi, T., 1981. The shape memory effect and related phenomena. In: Proceedings of the International Conference on Solid–Solid Phase Transformations, pp. 1455–1479, Carnegie–Mellon University, Pittsburgh, PA.
- Okamoto, K., Ichinose, S., Morii, K., Otsuka, K., Shimizu, K., 1986. Stress-induced martensitic transformation in a Cu–Al–Ni alloy. Acta Metal. 34, 2065–2073.
- Ortiz, M., Repetto, E., Stainier, L., 2000. A theory of subgrain dislocation structures. J. Mech. Phys. Solids 48, 2077–2114.
- Pagano, S., Alert, P., Maisonneuve, O., 1998. Solid–solid phase transition modelling. Local and global minimizations of non-convex and relaxed potentials. Isothermal case for shape memory alloys. Int. J. Eng. Sci. 36, 1143–1172.
- Roubicek, T., 2001. Evolution model for martensitic phase transformations in shape-memory alloys. Interfaces Free Boundaries, to appear.
- Sands, D., 1975. Introduction to Crystallography. Dover Publications, New York.
- Shield, T., 1995. Orientation dependence of the pseudoelastic behavior of single crystals of Cu–Al–Ni in tension. J. Mech. Phys. Solids 43, 869–895.
- Smyshlyaev, V., Willis, J., 1998. On the relaxation of a three-well energy. Proc. R. Soc. London A 455, 779–814.
- Tartar, L., 1990. H-measures, a new approach for studying homogenization, oscillation and concentration effects in partial differential equations. Proc. R. Soc. Edinburgh A 115, 193–230.
- Theil, F., 2002. Relaxation of rate independent evolution problems. Proc. R. Soc. Edinburgh A, in press.